Bayesian Methods for Updating Dynamic Models

Ka-Veng Yuen

Sin-Chi Kuok

Department of Civil and Environmental Engineering,
Faculty of Science and Technology,
University of Macau,
Macao, China

Model updating of dynamical systems has been attracting much attention because it has a very wide range of applications in aerospace, civil, and mechanical engineering, etc. Many methods were developed and there has been substantial development in Bayesian methods for this purpose in the recent decade. This article introduces some state-of-the-art work. It consists of two main streams of model updating, namely model updating using response time history and model updating using modal measurements. The former one utilizes directly response time histories for the identification of uncertain parameters. In particular, the Bayesian time-domain approach, Bayesian spectral density approach and Bayesian fast Fourier transform approach will be introduced. The latter stream utilizes modal measurements of a dynamical system. The method introduced here does not require a mode matching process that is common in other existing methods. Afterwards, discussion will be given about the relationship among model complexity, data fitting capability and robustness. An application of a 22-story building will be presented. Its acceleration response time histories were recorded during a severe typhoon and they are utilized to identify the fundamental frequency of the building. Furthermore, three methods are used for analysis on this same set of measurements and comparison will be made. [DOI: 10.1115/1.4004479]

1 Introduction

The problem of parametric identification for mathematical models using input-output or output-only dynamic measurements has received much attention over the years [1–12]. One important special case is modal identification, in which the parameters for identification are the small-amplitude modal frequencies, damping ratios, mode shapes and modal participation factors of the lower modes of the dynamical system [13–15]. In particular, model updating of mechanical or structural systems using ambient vibration survey is important. It has attracted much interest because it offers a means of obtaining dynamic data in an economical and efficient manner, without requiring the setup of special dynamic experiments (e.g., actuators) which are usually costly, time consuming, and often obtrusive [16–18]. In ambient vibration survey, the naturally occurring vibration of the structure is measured under wind, traffic, and micro-tremors, etc. Then, a system identification technique is used to identify the small-amplitude modal frequencies, damping ratios and mode shapes of the lower modes of the structure [19]. The assumption usually made is that the input excitation is a broad-band stochastic process adequately modeled as stationary Gaussian white noise. A number of methods have been developed to tackle this problem, e.g., the instrumental variable method [20], the eigensystem realization algorithm [21], the random decrement technique [22], the novelty measure technique [23] and the natural excitation technique [24]. Several other methods are based on fitting the correlation functions using least-squares type of approach [25,26]. Different ARMA model based least-squares methods have also been proposed, e.g., the two-stage least-squares method [27–29]. Another important type of methods is the prediction error methods [30–32] that minimize the optimally selected one-step-ahead output prediction error. The possible usage of Kalman filter for model identification was recognized in Ref. [33]. In Ref. [34], the extended Kalman filter was investigated for the applications to estimate the dynamic properties, such as modal frequencies, modal damping coefficients and participation factors, of linear multidegree-of-freedom systems. Since then, many methods were proposed as its evolution for linear and nonlinear dynamical systems [35–44]. Other nonlinear system identification methods based on advanced statistical tools (such as wavelets, higher-order spectra, Lie series, and artificial neural networks) have also been investigated for the case of known input [45–50] and for the case of unknown input [51–54].

Results of modal/model identification are usually restricted to the optimal values of the uncertain parameters. However, there is additional information related to the uncertainty associated with the parameter estimates and it is valuable for further processing. For example, in the case where the identified modal parameters are used to update the theoretical finite-element model of a structure, the updating procedure involves the minimization of a positive definite quadratic function of the differences between the theoretical and the experimental modal parameters. The weighting matrix in this goodness-of-fit function should reflect the uncertainty in the values of the identified modal parameters so it can be chosen as the inverse of the covariance matrix of these parameters. In practice, this covariance matrix is usually estimated by computing the statistics of the optimal estimates of the modal parameters from several sets of ambient data. However, this estimation is unreliable unless the number of data sets is large. Recent interest has been arisen to determine the uncertainty of the identified parameters of mechanical/structural systems using Bayesian probabilistic approach [55–87]. The parametric uncertainty can be quantified in the form of probability distribution in Bayesian inference [88,89]. The quantified uncertainty can be utilized for post-processing, such as probabilistic control [90–92]. In this paper, some state-of-the-art Bayesian methods are introduced. First, an exact formulation with output-only data is presented and its computational difficulty will be discussed. Then, the general model updating problem will be formulated in Sec. 3. In parametric identification or model updating, a given model class with uncertain parameters is prescribed and identification techniques are used to identify these uncertain parameters. Two important problems in structural dynamics are introduced in Secs. 4 and 5. In Sec. 4, model updating using measured response of the underlying system is considered. A method with input-output measurement will be introduced. Its extension for explicit consideration of both input and output noise is also presented. Then, in the second part of this section, the Bayesian time-domain method, Bayesian spectral density method and Bayesian fast Fourier transform method will be presented for output-only measurement. In Sec. 5, another important type of model updating problem using identified eigenvalues and eigenvectors of the system is introduced. The method presented here does not require model matching, which is necessary in most existing methods but difficult in some practical situation. After introducing parametric identification techniques, Sec. 6 discusses some of the key issues of model updating, including data fitting capability, robustness and posterior uncertainty. Finally, an example of structural health monitoring under severe typhoon is

Manuscript received October 26, 2010; final manuscript received May 31, 2011; published online September 26, 2011. Transmitted by Assoc. Editor: Chin An Tan.

 Copyright © 2011 by ASME

Downloaded 29 Sep 2011 to 161.64.70.118. Redistribution subject to ASME license or copyright; see http://www.asme.org/terms/Terms_Use.cfm

demonstrated in Sec. 7. The data will be analyzed by three methods and comparison will be given.

2 Exact Bayesian Formulation and Its Computational Difficulties

Consider a single-degree-of-freedom (SDOF) system with equation of motion:

$$\ddot{x} + 2\zeta\Omega\dot{x} + \Omega^2 x = f(t) \tag{1}$$

where Ω and ζ are the natural frequency and damping ratio of the oscillator, respectively. The input f is modeled as a zero-mean stationary Gaussian white noise with spectral intensity S_{f0}. Assuming stationarity of the response x, it is Gaussian with zero-mean and autocorrelation function

$$R_x(\tau) = \frac{\pi S_{f0}}{2\zeta\Omega^3}\exp(-\zeta\Omega|\tau|)\left[\cos(\Omega_d\tau) + \frac{\zeta}{\sqrt{1-\zeta^2}}\sin(\Omega_d|\tau|)\right] \tag{2}$$

where $\Omega_d = \Omega\sqrt{1-\zeta^2}$ is the damped natural frequency of the oscillator [93,94]

Discrete data is sampled with time step Δt and use y_n to denote the measured response at time $t = n\Delta t$. Due to measurement noise and modeling error, there is a difference between the measured response y_n and the model response $x(n\Delta t)$, referred to hereafter as prediction error. It is assumed that the prediction error can be adequately represented by a discrete white noise process ε with zero mean and variance σ_ε^2:

$$y_n = x(n\Delta t) + \varepsilon_n, \quad n = 1, 2, \ldots, N \tag{3}$$

so this process ε satisfies $E[\varepsilon_n\varepsilon_{n'}] = \sigma_\varepsilon^2\delta_{nn'}$, where $\delta_{nn'}$ denotes the Kronecker delta. Furthermore, the stochastic response x and prediction error ε are assumed statistically independent.

Therefore, the set of measurement D includes the data points, $y_1, y_2, \ldots, y_N$, and define a column vector: $\mathbf{Y} = [y_1, y_2, \ldots, y_N]^T$. It follows that the likelihood function for a given set of data D is given by

$$p(D|\boldsymbol{\theta}, C) = (2\pi)^{-\frac{N}{2}}|\Gamma(\boldsymbol{\theta})|^{-\frac{1}{2}}\exp\left[-\frac{1}{2}\mathbf{Y}^T\Gamma(\boldsymbol{\theta})^{-1}\mathbf{Y}\right] \tag{4}$$

where C is the prescribed class of models governed by Eq. (1) with the parameterization $\boldsymbol{\theta} = [\Omega, \zeta, S_{f0}, \sigma_\varepsilon]^T$ for the dynamical model to be identified. The notation $|\mathbf{A}|$ is used to denote the determinant of a matrix $\mathbf{A}$. The likelihood function $p(D|\boldsymbol{\theta}, C)$ is an N-variate Gaussian distribution of the measurement vector $\mathbf{Y}$ with zero mean and covariance matrix $\Gamma(\boldsymbol{\theta})$ with the (n,n') element $\Gamma^{(n,n')}(\boldsymbol{\theta}) \equiv E[y_n y_{n'}]$ is given by

$$\Gamma^{(n,n')}(\boldsymbol{\theta}) = R_x[(n-n')\Delta t|\boldsymbol{\theta}] + \sigma_\varepsilon^2\delta_{nn'} \tag{5}$$

where R_x is the autocorrelation function of the system response for a given model parameter vector $\boldsymbol{\theta}$ and it is given by Eq. (2).

However, for a large number of observed data points, repeated evaluations of the likelihood function $p(D|\boldsymbol{\theta}, C)$ for different values of $\boldsymbol{\theta}$ become computationally prohibitive. This is obvious from Eq. (4) that it requires the computation of the solution $\mathbf{X}$ of the algebraic equation $\Gamma(\boldsymbol{\theta})\mathbf{X} = \mathbf{Y}$ and the determinant of the $N \times N$ matrix $\Gamma(\boldsymbol{\theta})$. This task is computationally very expensive for large number of data points N. Repeated evaluations of the likelihood function for thousands times in the optimization process is computationally prohibitive even for a linear single-degree-of-freedom system. Therefore, the exact Bayesian approach described above, based on direct use of the measured data D, becomes practically infeasible.

3 Formulation of Model Updating Using Response Measurement

Consider a linear dynamical system with N_d degrees of freedom (DOFs) and its equation of motion is given by

$$\mathbf{M}\ddot{\mathbf{x}} + \mathbf{C}\dot{\mathbf{x}} + \mathbf{K}\mathbf{x} = \mathbf{T}_0\mathbf{F}(t) \tag{6}$$

where $\mathbf{M}$, $\mathbf{C}$ and $\mathbf{K}$ are the mass, damping and stiffness matrices, respectively; $\mathbf{T}_0 \in R^{N_d \times N_F}$ is a force distributing matrix; and the input $\mathbf{F}(t) \in R^{N_F}$ can be measured or unmeasured and that depends on the application.

Discrete data of a system response quantity $\mathbf{Q}$, e.g., acceleration, is taken at N_o $(\leq N_d)$ measured DOFs at times $t = n\Delta t$, $n = 1, 2, \ldots, N$. Also, due to measurement noise and modeling error, there is prediction error, i.e., a difference between the measured response $\mathbf{y}_n \in R^{N_o}$ and the model response at time $t = n\Delta t$ corresponding to the measured degrees of freedom. The latter is given by $\mathbf{Q}(n\Delta t)$. Therefore, the measured response $\mathbf{y}_n$ at time $n\Delta t$ can be expressed as follows:

$$\mathbf{y}_n = \mathbf{Q}(n\Delta t) + \boldsymbol{\varepsilon}_n \tag{7}$$

It is assumed that the prediction error can be adequately represented by a discrete zero-mean Gaussian white noise $\boldsymbol{\varepsilon}$ with the following $N_o \times N_o$ covariance matrix:

$$E\left[\boldsymbol{\varepsilon}_n\boldsymbol{\varepsilon}_{n'}^T\right] = \Sigma_\varepsilon\delta_{nn'} \tag{8}$$

where $\delta_{nn'}$ is the Kronecker delta. Furthermore, the prediction error $\boldsymbol{\varepsilon}$ and the stochastic response $\mathbf{Q}$ are assumed statistically independent.

Use $\boldsymbol{\theta}$ to denote the uncertain parameter vector that determines the dynamical model within a prescribed class of models C. These parameters include: (i) the structural parameters that determine the model matrices $\mathbf{M}$, $\mathbf{C}$ and $\mathbf{K}$; (ii) the forcing parameters defining the stochastic model of the input if it is treated as a stochastic process; (iii) the parameters defining the stochastic properties of the measurement noise. Herein, the identification of the model parameter vector $\boldsymbol{\theta}$ given some measured data D is concerned. Using the Bayes' theorem, the posterior/updated probability density function (PDF) of the model parameter vector $\boldsymbol{\theta}$ is given by

$$p(\boldsymbol{\theta}|D, C) = \kappa_1 p(\boldsymbol{\theta}|C)p(D|\boldsymbol{\theta}, C) \tag{9}$$

where κ_1 is the normalizing constant such that integrating the right hand side over the parameter space yields unity. The prior PDF $p(\boldsymbol{\theta}|C)$ reflects the prior information of the parameters without using the data. The likelihood function $p(D|\boldsymbol{\theta}, C)$ is the dominant factor when the number of data points is large. It reflects the contribution of the measured data D in establishing the updated PDF of the parameters. The relative plausibility between two values of $\boldsymbol{\theta}$ does not depend on the normalizing constant κ_1. It depends only on the relative values of the product of the prior PDF $p(\boldsymbol{\theta}|C)$ and likelihood function $p(D|\boldsymbol{\theta}, C)$. In order to search for the most probable model parameter vector $\boldsymbol{\theta}$, denoted by $\boldsymbol{\theta}^*$, one minimizes the objective function: $J(\boldsymbol{\theta}) = -\ln[p(\boldsymbol{\theta}|C)\, p(D|\boldsymbol{\theta}, C)]$, which is the negative logarithm of the product of the prior PDF and the likelihood function.

The reason for minimizing the objective function $J(\boldsymbol{\theta})$ instead of maximizing the posterior PDF directly is that the former has better computational condition. It is found that the updated PDF of the parameter vector $\boldsymbol{\theta}$ can be well approximated by a Gaussian distribution with mean $\boldsymbol{\theta}^*$ and covariance matrix $\mathcal{H}(\boldsymbol{\theta}^*)^{-1}$, where $\mathcal{H}(\boldsymbol{\theta}^*)$ denotes the Hessian of the objective function $J(\boldsymbol{\theta})$ calculated at $\boldsymbol{\theta} = \boldsymbol{\theta}^*$.

4 Bayesian Model Updating Using Response Measurements

4.1 Input-Output Data

4.1.1 Noise-Free Input Measurement. In this section, a method is introduced to utilize input-output measurement for identification purpose. The input measurement is considered noise free so the uncertain parameter vector $\boldsymbol{\theta}$ includes the model parameters $\boldsymbol{\theta}_m$ and the parameters that determine the elements of the upper right triangular part of the prediction-error covariance matrix Σ_ε (symmetry defines the lower triangular part of this matrix). The dynamic data D consists of the measured time histories at N discrete time steps of the excitation and system response. Assume equal variances and stochastic independence for the prediction

Downloaded 29 Sep 2011 to 161.64.70.118. Redistribution subject to ASME license or copyright; see http://www.asme.org/terms/Terms_Use.cfm

errors of different channels of measurements so the covariance matrix for the prediction errors is $\Sigma_\varepsilon = \sigma_\varepsilon^2 \mathbf{I}_{N_o}$, where $\mathbf{I}_{N_o}$ is the $N_o \times N_o$ identity matrix. Then, the updated PDF of the uncertain parameters in $\boldsymbol{\theta} = [\boldsymbol{\theta}_m^T, \sigma_\varepsilon^2]^T$ given the data D and model class C can be expressed as

$$p(\boldsymbol{\theta}|D,C) = \kappa_2 p(\boldsymbol{\theta}|C)(2\pi)^{-\frac{NN_o}{2}} \sigma_\varepsilon^{-NN_o} \exp\left[-\frac{NN_o}{2\sigma_\varepsilon^2} J_g(\boldsymbol{\theta}_m; D, C)\right] \tag{10}$$

where κ_2 is a normalizing constant and $p(\boldsymbol{\theta}|C)$ is the prior PDF of the uncertain parameters in $\boldsymbol{\theta}$, expressing the user's judgment about the relative plausibility of the values of the uncertain parameters before the data are used. The goodness-of-fit function is given by [58,95,96]

$$J_g(\boldsymbol{\theta}_m; D, C) = \frac{1}{NN_o} \sum_{n=1}^{N} \left\| \mathbf{y}_n - \mathbf{Q}(n\Delta t; \boldsymbol{\theta}_m, C) \right\|^2 \tag{11}$$

where $\mathbf{Q}(n\Delta t; \boldsymbol{\theta}_m, C)$ is the model response based on the assumed class of models and the model parameter vector $\boldsymbol{\theta}_m$ while $\mathbf{y}_n$ is the measured response at time $n\Delta t$. Furthermore, $||.||$ denotes the Euclidean norm (2-norm) of a vector. The most probable model parameter vector $\boldsymbol{\theta}_m^*$ is obtained by maximizing the posterior PDF in Eq. (10). For large N or with improper prior, this is equivalent to minimizing the goodness-of-fit function $J_g(\boldsymbol{\theta}_m; D, C)$ in Eq. (11) over all possible values of $\boldsymbol{\theta}_m$:

$$\boldsymbol{\theta}_m^* = \arg\min_{\boldsymbol{\theta}_m} J_g(\boldsymbol{\theta}_m; D, C) \tag{12}$$

If $J_g(\boldsymbol{\theta}_m; D, C)$ is known only implicitly, numerical optimization is needed to search for the optimal model parameters and this can be done by the function 'fminsearch' in MATLAB. The most probable value of the prediction-error variance in $\boldsymbol{\theta}^*$ can be obtained also by maximizing the posterior PDF and the solution is available in closed form:

$$\sigma_\varepsilon^{2*} = \min_{\boldsymbol{\theta}_m} J_g(\boldsymbol{\theta}_m; D, C) = \min_{\boldsymbol{\theta}_m} J_g(\boldsymbol{\theta}_m^*; D, C) \tag{13}$$

For dynamic testing, it is the number of observed degrees of freedom, N_o, and their distribution that are the essential factors for identifiability. On the other hand, increasing the number data points N does not increase the number of effective mathematical constraints, and hence the identifiability.

For globally model-identifiable cases with large N [97,98], it turns out that the posterior PDF $p(\boldsymbol{\theta}|D,C)$ is approximately Gaussian. The mean is the optimal parameter vector $\boldsymbol{\theta}^*$ and the covariance matrix is equal to the inverse of the Hessian matrix of the objective function $J(\boldsymbol{\theta}) = -\ln[p(D|\boldsymbol{\theta},C)p(\boldsymbol{\theta}|C)]$ at $\boldsymbol{\theta}^*$:

$$\mathcal{H}^{(l,l')}(\boldsymbol{\theta}^*) = -\frac{\partial^2}{\partial\theta_l \partial\theta_{l'}} \ln[p(D|\boldsymbol{\theta},C)p(\boldsymbol{\theta}|C)]|_{\boldsymbol{\theta}=\boldsymbol{\theta}^*} \tag{14}$$

Since the uncertainty of the estimation can be quantified, the optimal sensor locations can be obtained using the information entropy [99] as a measure of the uncertainty of multivariate random variables [100–104].

In practice, the prior distribution may be used as a regularizer [105,106] to improve the well-posedness of the inverse problem:

$$p(\boldsymbol{\theta}|C) = (2\pi)^{-\frac{N_\theta}{2}} \left(\prod_{l=1}^{N_\theta} \sigma_l\right) \exp\left(-\frac{1}{2}\sum_{l=1}^{N_\theta} \frac{\theta_l^2}{\sigma_l^2}\right) \tag{15}$$

It is a Gaussian PDF with zero mean so it decays as the radial distance to the origin increases in any direction. If there exist two or more sets of parameters to give the same likelihood function values, using this radially decaying prior distribution helps trimming down the set of the optimal parameters to the one with the smallest 2-norm.

4.1.2 Consideration With Input Measurement Noise. In the above method, it is assumed that there is no measurement error in the input. Here, a method is introduced to consider explicitly the measurement noise in both the input and output data. This feature avoids the possible underestimation on the parametric uncertainty in practice. Let N denote the total number of observed time steps. Using the Bayes' theorem, the updated PDF of the parameters $\boldsymbol{\theta}$ given the measured input $\mathbf{G}_1, \mathbf{G}_2, \ldots, \mathbf{G}_N$ of the excitation $\mathbf{F}$ and the measured response $\mathbf{y}_1, \mathbf{y}_2, \ldots, \mathbf{y}_N$ is given by

$$\begin{aligned} p(\boldsymbol{\theta}|\mathbf{y}_1, \mathbf{y}_2, \ldots, \mathbf{y}_N, \mathbf{G}_1, \mathbf{G}_2, \ldots, \mathbf{G}_N, C) \\ = \kappa_3 p(\boldsymbol{\theta}|\mathbf{G}_1, \mathbf{G}_2, \ldots, \mathbf{G}_N, C) \\ \times p(\mathbf{y}_1, \mathbf{y}_2, \ldots, \mathbf{y}_N|\mathbf{G}_1, \mathbf{G}_2, \ldots, \mathbf{G}_N, \boldsymbol{\theta}, C) \end{aligned} \tag{16}$$

where κ_3 is a normalizing constant. The probability distribution $p(\boldsymbol{\theta}|\mathbf{G}_1, \mathbf{G}_2, \ldots, \mathbf{G}_N, C)$ represents the information from the measured input only. It can be approximated by the prior PDF $p(\boldsymbol{\theta}|\mathbf{G}_1, \mathbf{G}_2, \ldots, \mathbf{G}_N, C) \approx p(\boldsymbol{\theta}|C)$ since the measured input alone does not have much saying on the model parameters (though it contains some information of the prediction-error variance, e.g., the root-mean-square (rms) of the measurement noise should be less than the rms of the measurement). The likelihood function $p(\mathbf{y}_1, \mathbf{y}_2, \ldots, \mathbf{y}_N|\mathbf{G}_1, \mathbf{G}_2, \ldots, \mathbf{G}_N, \boldsymbol{\theta}, C)$ reflects the contribution of the measured data $\mathbf{y}_1, \mathbf{y}_2, \ldots, \mathbf{y}_N$ and $\mathbf{G}_1, \mathbf{G}_2, \ldots, \mathbf{G}_N$ in establishing the updated PDF of the model parameters. Since $p(\mathbf{y}_1, \mathbf{y}_2, \ldots, \mathbf{y}_N|\mathbf{G}_1, \mathbf{G}_2, \ldots, \mathbf{G}_N, \boldsymbol{\theta}, C)$ is jointly Gaussian, direct calculation of this PDF encounters similar computational problems as in the exact formulation shown in Sec. 2. Therefore, an approximated likelihood expansion is introduced [107]:

$$\begin{aligned} p(\mathbf{y}_1, \mathbf{y}_2, \ldots, \mathbf{y}_N|\mathbf{G}_1, \mathbf{G}_2, \ldots, \mathbf{G}_N, \boldsymbol{\theta}, C) \\ \approx p(\mathbf{y}_1, \mathbf{y}_2, \ldots, \mathbf{y}_{N_p}|\mathbf{G}_1, \mathbf{G}_2, \ldots, \mathbf{G}_N, \boldsymbol{\theta}, C) \\ \times \prod_{n=N_p+1}^{N} p(\mathbf{y}_n|\mathbf{y}_{n-N_p+1}, \ldots, \mathbf{y}_{n-1}, \mathbf{G}_1, \mathbf{G}_2, \ldots, \mathbf{G}_N, \boldsymbol{\theta}, C) \end{aligned} \tag{17}$$

The conditional PDFs are conditional on the last N_p time steps only. In order to obtain the reduced-order joint PDF and the conditional PDFs, the differential equation of the state space model was converted to a difference equation. By considering the input measurement noise, the usually observed problem of underestimating the parametric uncertainty can be resolved. The reduced-order likelihood function $p(\mathbf{y}_1, \mathbf{y}_2, \ldots, \mathbf{y}_{N_p}|\mathbf{G}_1, \mathbf{G}_2, \ldots, \mathbf{G}_N, \boldsymbol{\theta}, C)$ and the conditional PDFs can be computed with the state space method described in Ref. [107].

In Ref. [108], the Bayesian unified approach was introduced to handle the more general case with incomplete input and incomplete output noisy measurements. The Bayesian unified method opens a wide range of applications, including the special cases of ambient vibration surveys, and measured input-output noisy data. An application was presented for a building subjected to wind and ground excitation simultaneously. The unmeasured wind pressure was modeled as a stochastic process with uncertain parameters but the ground excitation was observed with measurement noise. The structural response was also observed at a limited number of DOFs only. The unified method was applied successfully for model updating and damage detection purpose.

4.2 Output-Only Methods

4.2.1 Bayesian Time-Domain Approach. Difficulty here is to construct the likelihood $p(D|\boldsymbol{\theta},C)$ because the random components of the data points are correlated, which is in contrast to the case with input-output data. By using the Bayes' theorem, the likelihood function can be expanded to a product of conditional PDFs and a reduced-order joint PDF [109]:

$$p(D|\boldsymbol{\theta},C) = p(\mathbf{y}_1, \mathbf{y}_2, \ldots, \mathbf{y}_{N_p}|\boldsymbol{\theta},C) \prod_{n=N_p+1}^{N} p(\mathbf{y}_n|\mathbf{y}_1, \mathbf{y}_2, \ldots, \mathbf{y}_{n-1}, \boldsymbol{\theta}, C) \tag{18}$$

This expansion is exact but it does not resolve the computational difficulties encountered in the exact formulation. This is because

Downloaded 29 Sep 2011 to 161.64.70.118. Redistribution subject to ASME license or copyright; see http://www.asme.org/terms/Terms_Use.cfm

the computation of each of the conditional PDFs $p(\mathbf{y}_n|\mathbf{y}_1, \mathbf{y}_2, \ldots, \mathbf{y}_{n-1}, \boldsymbol{\theta}, C)$ for large n requires similar computational effort as in the computation of the likelihood function $p(D|\boldsymbol{\theta}, C)$ in the direct exact formulation and the right hand side of the expansion involves many such conditional PDFs. In order to overcome this computational obstacle, the following approximation for the likelihood function is introduced [110]:

$$p(D|\boldsymbol{\theta}, C) \approx p(\mathbf{y}_1, \mathbf{y}_2, \ldots, \mathbf{y}_{N_p}|\boldsymbol{\theta}, C) \times \prod_{n=N_p+1}^{N} p(\mathbf{y}_n|\mathbf{y}_{n-N_p}, \mathbf{y}_{n-N_p+1}, \ldots, \mathbf{y}_{n-1}, \boldsymbol{\theta}, C) \quad (19)$$

In other words, the conditional PDFs depending on more than N_p previous data points are approximated by the conditional PDFs depending on only the last N_p data points. The sense of this approximation is that data points belonging too far in the past do not have significant information on the system response of the present point. Of course, one expects this to be legitimate, if N_p is so large that the correlation functions have decayed to negligible values. However, it is sufficient to use a value of N_p to include the data points within one fundamental period of the oscillator. In other words, the value of N_p is chosen to cover roughly one fundamental period of the system. In the case of multidegree-of-freedom systems (i.e., multimode systems), such a selected value of N_p covers more than one period of the higher modes so the approximation is even more accurate for the higher modes. Although the fundamental frequency Ω is an unknown parameter, it can be roughly estimated from the first peak of the response spectrum to obtain the value of N_p prior to the identification. The identification result is not sensitive to the selected value of N_p if it is sufficiently large.

Use $\mathbf{Y}_{n,n'}$ to denote the vector comprised of the response measurements from time $n\Delta t$ to $n'\Delta t$ $(n \le n')$ in a time-descending order:

$$\mathbf{Y}_{n,n'} = \left[\mathbf{y}_{n'}^T, \mathbf{y}_{n'-1}^T, \ldots, \mathbf{y}_n^T\right]^T, \quad n \le n' \quad (20)$$

Then, the joint PDF $p(\mathbf{y}_1, \mathbf{y}_2, \ldots, \mathbf{y}_{N_p}|\boldsymbol{\theta}, C)$ follows an $N_o N_p$ -variate Gaussian distribution with zero mean and covariance matrix $\Sigma_{Y_{1,N_p}}$:

$$\Sigma_{Y_{1,N_p}} = E[\mathbf{Y}_{1,N_p}\mathbf{Y}_{1,N_p}^T] = \begin{bmatrix} \Gamma_{N_p,N_p} & & sym \\ \vdots & \ddots & \\ \Gamma_{1,N_p} & \cdots & \Gamma_{1,1} \end{bmatrix} \quad (21)$$

where the submatrix $\Gamma_{n,n'}$ has dimension $N_o \times N_o$ and it is given by

$$\Gamma_{n,n'} = E\left[\mathbf{y}_n\mathbf{y}_{n'}^T\right] = \mathbf{R}_Q(n\Delta t, n'\Delta t) + \Sigma_\varepsilon \delta_{nn'} \quad (22)$$

where $\delta_{nn'}$ is the Kronecker Delta; $\mathbf{R}_Q$ denotes the autocorrelation matrix function of the model response $\mathbf{Q}$; and Σ_ε is the noise covariance matrix defined in Eq. (8). Since the random vectors $\mathbf{y}_1, \mathbf{y}_2, \ldots, \mathbf{y}_{N_p}$ are jointly Gaussian with zero mean, the reduced-order likelihood function $p(\mathbf{y}_1, \mathbf{y}_2, \ldots, \mathbf{y}_{N_p}|\boldsymbol{\theta}, C)$ is given by

$$p(\mathbf{y}_1, \mathbf{y}_2, \ldots, \mathbf{y}_{N_p}|\boldsymbol{\theta}, C) = (2\pi)^{-\frac{N_o N_p}{2}}|\Sigma_{Y_{1,N_p}}|^{-\frac{1}{2}} \times \exp\left(-\frac{1}{2}\mathbf{Y}_{1,N_p}^T\Sigma_{Y_{1,N_p}}^{-1}\mathbf{Y}_{1,N_p}\right) \quad (23)$$

To compute this likelihood function, it involves only the solution of the linear algebraic equation $\Sigma_{Y_{1,N_p}}\mathbf{X} = \mathbf{Y}_{1,N_p}$ and the determinant of the matrix $\Sigma_{Y_{1,N_p}}$ which is $N_o N_p \times N_o N_p$ only.

Then, the general expression is given for the conditional probability densities involving N_p previous points $p(\mathbf{y}_n|\mathbf{y}_{n-N_p}, \mathbf{y}_{n-N_p+1}, \ldots, \mathbf{y}_{n-1}, \boldsymbol{\theta}, C)$ in Eq. (19), with $n > N_p \ge 1$. First, the random vector $\mathbf{Y}_{n-N_p,n}$ has zero mean and covariance matrix $\Sigma_{Y_{n-N_p,n}}$:

$$\Sigma_{Y_{n-N_p,n}} = E\left[\mathbf{Y}_{n-N_p,n}\mathbf{Y}_{n-N_p,n}^T\right] = \begin{bmatrix} \Gamma_{n,n} & & sym \\ \vdots & \ddots & \\ \Gamma_{n-N_p,n} & \cdots & \Gamma_{n-N_p,n-N_p} \end{bmatrix} \quad (24)$$

where the submatrix $\Gamma_{n,n'}$ is given by Eq. (22). Then, this matrix is partitioned as follows:

$$\Sigma_{Y_{n-N_p,n}} = \begin{bmatrix} \Sigma_{11,n} & \Sigma_{12,n} \\ \Sigma_{12,n}^T & \Sigma_{22,n} \end{bmatrix} \quad (25)$$

where the matrices $\Sigma_{11,n}$, $\Sigma_{12,n}$ and $\Sigma_{22,n}$ have dimensions $N_o \times N_o$, $N_o \times N_o N_p$ and $N_o N_p \times N_o N_p$, respectively. $\Sigma_{11,n}$ and $\Sigma_{22,n}$ are the unconditional covariance matrix of the prediction target variables and the conditioning variables; and the matrix $\Sigma_{12,n}$ quantifies their correlation.

Since the measured response has zero mean, the optimal estimator $\hat{\mathbf{y}}_n$ of $\mathbf{y}_n$ conditional on $\mathbf{Y}_{n-N_p,n-1}$ is given by [111]:

$$\hat{\mathbf{y}}_n \equiv E\lfloor \mathbf{y}_n|\mathbf{y}_{n-N_p}, \mathbf{y}_{n-N_p+1}, \ldots, \mathbf{y}_{n-1}, \boldsymbol{\theta}, C\rfloor = \Sigma_{12,n}\Sigma_{22,n}^{-1}\mathbf{Y}_{n-N_p,n-1} \quad (26)$$

and the covariance matrix $\Sigma_{e,n}$ of the prediction error $\mathbf{e}_n = \mathbf{y}_n - \hat{\mathbf{y}}_n$ is given by

$$\Sigma_{e,n} \equiv E\lfloor \mathbf{e}_n\mathbf{e}_n^T|\mathbf{y}_{n-N_p}, \mathbf{y}_{n-N_p+1}, \ldots, \mathbf{y}_{n-1}, \boldsymbol{\theta}, C\rfloor = \Sigma_{11,n} - \Sigma_{12,n}\Sigma_{22,n}^{-1}\Sigma_{12,n}^T \quad (27)$$

Therefore, the conditional probability density $p(\mathbf{y}_n|\mathbf{y}_{n-N_p}, \mathbf{y}_{n-N_p+1}, \ldots, \mathbf{y}_{n-1}, \boldsymbol{\theta}, C)$ follows an N_o-variate Gaussian distribution with mean $\hat{\mathbf{y}}_n$ and covariance matrix $\Sigma_{e,n}$:

$$p(\mathbf{y}_n|\mathbf{y}_{n-N_p}, \mathbf{y}_{n-N_p+1}, \ldots, \mathbf{y}_{n-1}, \boldsymbol{\theta}, C) = (2\pi)^{-\frac{N_o}{2}}|\Sigma_{e,n}|^{-\frac{1}{2}}\exp\left[-\frac{1}{2}(\mathbf{y}_n - \hat{\mathbf{y}}_n)^T\Sigma_{e,n}^{-1}(\mathbf{y}_n - \hat{\mathbf{y}}_n)\right] \quad (28)$$

The most probable parameter vector $\boldsymbol{\theta}^*$ is obtained by minimizing the objective function which is the negative logarithm of the posterior PDF (without including the terms that do not depend on $\boldsymbol{\theta}$):

$$J(\boldsymbol{\theta}) = -\ln p(\boldsymbol{\theta}|C) + \frac{1}{2}\ln|\Sigma_{Y_{1,N_p}}| + \frac{1}{2}\mathbf{Y}_{1,N_p}^T\Sigma_{Y_{1,N_p}}^{-1}\mathbf{Y}_{1,N_p} + \frac{1}{2}\sum_{n=N_p+1}^{N}\left[\ln|\Sigma_{e,n}| + (\mathbf{y}_n - \hat{\mathbf{y}}_n)^T\Sigma_{e,n}^{-1}(\mathbf{y}_n - \hat{\mathbf{y}}_n)\right] \quad (29)$$

In the special case of stationary response, the matrices $\Sigma_{e,n} = \Sigma_e$ and $\Sigma_{12,n}\Sigma_{22,n}^{-1} = \Sigma_{12}\Sigma_{22}^{-1}$ required in the computation of the optimal estimator $\hat{\mathbf{y}}_n$ do not depend on the time step n. Therefore, the objective function in Eq. (29) can be simplified as follows:

$$J(\boldsymbol{\theta}) = -\ln p(\boldsymbol{\theta}|C) + \frac{1}{2}\ln|\Sigma_{Y_{1,N_p}}| + \frac{1}{2}\mathbf{Y}_{1,N_p}^T\Sigma_{Y_{1,N_p}}^{-1}\mathbf{Y}_{1,N_p} + \frac{N-N_p}{2}\ln|\Sigma_e| + \frac{1}{2}\sum_{n=N_p+1}^{N}(\mathbf{y}_n - \hat{\mathbf{y}}_n)^T\Sigma_e^{-1}(\mathbf{y}_n - \hat{\mathbf{y}}_n) \quad (30)$$

In this case, it requires only the computation of the inverse and determinant of the matrices $\Sigma_{Y_{1,N_p}}$ $(=\Sigma_{22,n})$ and Σ_e, which are $N_o N_p \times N_o N_p$, and $N_o \times N_o$, respectively. These sizes are much smaller than the $NN_o \times NN_o$ matrix $\Sigma_{Y_{1,N}}$ appeared in the direct formulation.

4.2.2 Bayesian Spectral Density Approach. The Bayesian spectral density approach is a frequency-domain approach. First, consider a discrete stochastic vector process $\mathbf{y}$ and a finite number

Downloaded 29 Sep 2011 to 161.64.70.118. Redistribution subject to ASME license or copyright; see http://www.asme.org/terms/Terms_Use.cfm

of discrete data points $D=\{\mathbf{y}_n, n=1,2,\ldots,N\}$. Based on D a discrete estimator of the spectral density matrix of the stochastic process y is introduced:

$$\mathbf{S}_{y,N}(\omega_k) = Y(\omega_k)Y(\omega_k)^H \tag{31}$$

where ^{H} denotes the adjoint or conjugate transpose of a complex vector/matrix. The vector $Y(\omega_k) \in C^{N_o}$ denotes the scaled discrete Fourier transform of the vector process $\mathbf{y}$ at frequency ω_k:

$$Y(\omega_k) = \sqrt{\frac{\Delta t}{2\pi N}} \sum_{n=0}^{N-1} \mathbf{y}_n \exp(-in\omega_k \Delta t) \tag{32}$$

where $\omega_k = k\Delta\omega, \quad k = 0, 1, \ldots, N_{nqy}$ with $N_{nqy} = INT(N/2)$, $\Delta\omega = 2\pi/T$, and $T = N\Delta t$.

Taking expectation of Eq. (31) yields

$$E[\mathbf{S}_{y,N}(\omega_k)|\boldsymbol{\theta}, C] = E[\mathbf{S}_{Q,N}(\omega_k)|\boldsymbol{\theta}, C] + E[\mathbf{S}_{\varepsilon,N}(\omega_k)|\boldsymbol{\theta}, C] \tag{33}$$

The matrices $\mathbf{S}_{Q,N}(\omega_k)$ and $\mathbf{S}_{\varepsilon,N}(\omega_k)$ are defined in similar manner to Eq. (31) and Eq. (32) for the vector processes $\mathbf{Q}$ and $\boldsymbol{\varepsilon}$, respectively. One can show that the first term on the right hand side has the following form [112]:

$$E[S_{Q,N}^{(l,l')}(\omega_k)|\boldsymbol{\theta}, C] = \frac{\Delta t}{2\pi N}\left[NR_Q^{(l,l')}(0) + \sum_{n=1}^{N-1}(N-n) \times \left[R_Q^{(l,l')}(n\Delta t)e^{in\omega_k\Delta t} + R_Q^{(l',l)}(n\Delta t)e^{-in\omega_k\Delta t}\right]\right] \tag{34}$$

where $\mathbf{R}_Q$ is the correlation matrix function of the quantity $\mathbf{Q}$. This estimator $E[S_{Q,N}^{(l,l')}(\omega_k)|\boldsymbol{\theta}, C]$ can be computed efficiently using the function 'fft' in Ref. [113]. For the measurement noise, since its correlation function is nonzero only with zero time lag, the term $E[\mathbf{S}_{\varepsilon,N}(\omega_k)|\boldsymbol{\theta}, C]$ can be readily obtained in terms of the covariance matrix Σ_ε:

$$E[\mathbf{S}_{\varepsilon,N}(\omega_k)|\boldsymbol{\theta}, C] = \frac{\Delta t}{2\pi}\Sigma_\varepsilon \equiv \mathbf{S}_{\varepsilon 0} \tag{35}$$

Assume that N_s sets of independent and identically distributed time histories are available: $D^{(1)}, D^{(2)}, \ldots, D^{(N_s)}$. As $T \to \infty$ and $\Delta t \to 0^+$, the corresponding discrete Fourier transforms $Y^{(s)}(\omega_k)$, $s = 1, 2, \ldots, N_s$, are independent and follow an identical complex N_o-variate normal distribution with zero mean. Then, the averaged spectral density matrix estimator:

$$\mathbf{S}_{y,N}^{av}(\omega_k) = \frac{1}{N_s}\sum_{s=1}^{N_s}\mathbf{S}_{y,N}^{(s)}(\omega_k) \tag{36}$$

follows the central complex Wishart distribution of dimension N_o with N_s degrees of freedom [114]. Its PDF is given by

$$p\left(\mathbf{S}_{y,N}^{av}(\omega_k)|\boldsymbol{\theta}, C\right) = \frac{\pi^{-\frac{N_o(N_o-1)}{2}} N_s^{N_o(N_s-N_o)} \left|\mathbf{S}_{y,N}^{av}(\omega_k)\right|^{N_s-N_o}}{\left(\prod_{s=1}^{N_o}(N_s-s)!\right)\left|E\left[\mathbf{S}_{y,N}(\omega_k)|\boldsymbol{\theta}, C\right]\right|^{N_s}} \times \exp\left(-N_s tr\left\{E\left[\mathbf{S}_{y,N}(\omega_k)|\boldsymbol{\theta}, C\right]^{-1}\mathbf{S}_{y,N}^{av}(\omega_k)\right\}\right) \tag{37}$$

where $|\mathbf{A}|$ and $\mathrm{tr}\{\mathbf{A}\}$ denote the determinant and trace of the matrix $\mathbf{A}$, respectively. Note that this PDF exists if and only if $N_s \geq N_o$. Furthermore, it can be shown that when $T \to \infty$ and $\Delta t \to 0^+$, the random matrices $\mathbf{S}_{y,N}^{av}(\omega_k)$ and $\mathbf{S}_{y,N}^{av}(\omega_{k'})$ are independently complex Wishart distributed for $k \neq k'$ [115].

Although the Wishart distribution and independence properties are exact only as $\Delta t \to 0^+$, it can be verified by simulation that they are good approximations in a particular frequency range. It was verified using simulation that such approximations are indeed accurate if an appropriately chosen bandwidth is considered. The reasons for the violation of these approximations are aliasing and leakage. Therefore, the range of frequency for accurate approximations is the region with large spectral values since the aliasing and leakage effects have relatively minor contribution in such frequency range. As a result, in the case of displacement measurement such range of frequencies corresponds to the lower frequency range. This range increases for higher levels of prediction error.

Based on the above discussion regarding the statistical properties of the averaged spectral estimator, the Bayesian spectral density approach for updating the uncertain parameter vector $\boldsymbol{\theta}$ is given as follows. With N_s $(\geq N_o)$ independent sets of observed data $D^{(s)}$, $s = 1, 2, \ldots, N_s$, the corresponding observed spectral density matrix estimators $\mathbf{S}_{y,N}^{(s)}(\omega_k)$, $s = 1, 2, \ldots, N_s$, $k \in \mathsf{K}$, can be obtained using Eq. (31) and Eq. (32). Then, the averaged spectral density matrix estimators $\mathbf{S}_{y,N}^{av}(\omega_k)$ is readily obtained by Eq. (36) to form the averaged spectral set: $S_{\mathsf{K}}^{av} \equiv \{\mathbf{S}_{y,N}^{av}(k\Delta\omega)|k \in \mathsf{K}\}$. Here, the frequency index set K represents a range over the Wishart distribution and independence approximations are satisfactory. Using the Bayes' theorem in a similar fashion as Eq. (9), the updated PDF of the model parameter vector $\boldsymbol{\theta}$ given the averaged spectral set S_{K}^{av} is given by

$$p(\boldsymbol{\theta}|S_{\mathsf{K}}^{av}, C) = \kappa_4 p(\boldsymbol{\theta}|C)p(S_{\mathsf{K}}^{av}|\boldsymbol{\theta}, C) \tag{38}$$

where κ_4 is a normalizing constant. The likelihood function $p(S_{\mathsf{K}}^{av}|\boldsymbol{\theta}, C)$ expresses the contribution of the measured data. Based on the Wishart distribution and independence approximation, it can be calculated as follows:

$$p\left(S_{\mathsf{K}}^{av}|\boldsymbol{\theta}, C\right) = \kappa_5 \prod_{k\in\mathsf{K}} \frac{1}{|E[\mathbf{S}_{y,N}(\omega_k)|\boldsymbol{\theta}, C]|^{N_s}} \times \exp(-N_s tr\{E[\mathbf{S}_{y,N}(\omega_k)]^{-1}\mathbf{S}_{y,N}^{av}(\omega_k)\}) \tag{39}$$

where

$$\kappa_5 = \pi^{-\frac{N_o(N_o-1)N_\omega}{2}}\left(\prod_{s=1}^{N_o}(N_s-s)!\right)^{-N_\omega} N_s^{N_o(N_s-N_o)N_\omega}\prod_{k\in\mathsf{K}}\left|\mathbf{S}_{y,N}^{av}(\omega_k)\right|^{N_s-N_o}$$

is a constant that does not depend on the uncertain parameters; N_ω is the number of frequency points to be considered and it is equal to the number of the distinct elements in the set K. For a given set of data, the constant κ_5 does not depend on the model parameters so it does not affect the optimal parameters and their associate uncertainties. Finally, the most probable parameter vector $\boldsymbol{\theta}^*$ is obtained by minimizing the objective function:

$$J(\boldsymbol{\theta}) = -\ln p(\boldsymbol{\theta} \mid C) + N_s \sum_{k\in\mathsf{K}}(\ln|E[\mathbf{S}_{y,N}(\omega_k)|\boldsymbol{\theta}, C]| + tr\{E[\mathbf{S}_{y,N}(\omega_k)]^{-1}\mathbf{S}_{y,N}^{av}(\omega_k)\}) \tag{40}$$

In the case if a noninformative prior is used, the first term can be simply neglected. Furthermore, the updated PDF of the parameter vector $\boldsymbol{\theta}$ can be well approximated by a Gaussian distribution with mean $\boldsymbol{\theta}^*$ and covariance matrix $\mathcal{H}(\boldsymbol{\theta}^*)^{-1}$, where $\mathcal{H}(\boldsymbol{\theta}^*)$ denotes the Hessian matrix of the objective function J calculated at $\boldsymbol{\theta} = \boldsymbol{\theta}^*$:

$$\mathcal{H}^{(l,l')}(\boldsymbol{\theta}^*) = N_s \sum_{k\in\mathsf{K}}\left[\frac{\partial^2}{\partial\theta_l\partial\theta_{l'}}(\ln|E[\mathbf{S}_{y,N}(\omega_k)|\boldsymbol{\theta}, C]| + tr\{E[\mathbf{S}_{y,N}(\omega_k)|\boldsymbol{\theta}, C]^{-1}\mathbf{S}_{y,N}^{av}(\omega_k)\})\right]_{\boldsymbol{\theta}=\boldsymbol{\theta}^*} - \left.\frac{\partial^2 \ln p(\boldsymbol{\theta}|C)}{\partial\theta_l\partial\theta_{l'}}\right|_{\boldsymbol{\theta}=\boldsymbol{\theta}^*} \tag{41}$$

The two approximations used in the Bayesian spectral density approach are accurate in a particular frequency range. It is

Downloaded 29 Sep 2011 to 161.64.70.118. Redistribution subject to ASME license or copyright; see http://www.asme.org/terms/Terms_Use.cfm

recommended to select the frequency index set to include only the range around the peaks in the spectrum even though the Chi-square/Wishart distribution and independence approximations are accurate over a wider range. This selection enhances the computational efficiency without sacrificing substantially the information for the frequency structure of the dynamical system (though it induces loss of information for the prediction-error variance). Another advantage is that the results by this choice will rely less on the whiteness assumption since it requires a flat spectral density function for each mode only around the corresponding peak instead of over the whole frequency range. Moreover, the aliasing and leakage effects generally have less influence on this range since their spectral values are large.

Another important advantage of this cutoff frequency range is as follows. In most existing probabilistic methods, the uncertainty of the model parameters will tend to zero if the sampling time interval tends to zero with a fixed observed duration (even if it is very short) as long as it is globally identifiable. This is the consequence of the discrete white noise assumption. Note that this phenomenon occurs even for filtered white noise, such as moving average or autoregressive output of white noise. However, for the Bayesian spectral density method with this proposed cutoff frequency range, the sampling time interval does not affect the frequency index set so the same number of frequencies is considered regardless of the sampling time interval (if it is sufficiently small). Therefore, the uncertainty of the model parameters estimated by the Bayesian spectral density method will stabilize as the sampling time step tends to zero. This feature of the methodology is appealing for practical purposes. Note that this method can be extended for nonlinear systems [116].

4.2.3 Bayesian Fast Fourier Transform Approach. The Bayesian fast Fourier transform approach uses the statistical properties of discrete Fourier transforms, instead of the spectral density estimators, to construct the likelihood function and the updated PDF of the model parameters [117]:

$$p(\mathrm{Y_K}|\boldsymbol{\theta},C) = k_6 \prod_{k\in \mathrm{K}} \frac{1}{(2\pi)^{N_o}\sqrt{|\Gamma_Z(\omega_k)|}} \times \exp\left(-\frac{1}{2}\mathbf{Z}(\omega_k)^T\Gamma_Z(\omega_k)^{-1}\mathbf{Z}(\omega_k)\right) \tag{42}$$

where $\mathrm{Y_K}$ denotes the set of discrete Fourier transform of the measurement defined in Eq. (32) in the frequency range described by the frequency index set K; the vector $\mathbf{Z}(\omega_k) = [\mathrm{Re}[\mathsf{Y}(\omega_k)]^T, \mathrm{Im}[\mathsf{Y}(\omega_k)]^T]^T$ is real and it includes the real and imaginary parts of the discrete Fourier transform; and the matrix $\Gamma_Z(\omega_k)$ is the covariance matrix of the vector $\mathbf{Z}(\omega_k)$ and its expression is given by Ref. [117].

This method does not rely on the approximation of the Wishart distributed spectrum and the individual Gaussian likelihood function given in Eq. (42) is exact. The only approximation was made on the independency of the discrete Fourier transforms at different frequencies. Therefore, the Bayesian fast Fourier transform approach is more accurate than the spectral density approach in the sense that one of the two approximations in the latter is released. However, since the fast Fourier transform approach considers the real and imaginary parts of the discrete Fourier transform, the corresponding covariance matrices are $2N_o \times 2N_o$, instead of $N_o \times N_o$ in the spectral density approach. Therefore, the spectral density approach is computationally more efficient than the fast Fourier transform approach.

4.2.4 Unknown Input Without Assuming its Stochastic Model. In the literature and the aforementioned identification methods, the input is either measured or modeled as a prescribed parametric stochastic model (even though the parameters may be unknown). This seems to be a necessary condition for model identification purpose. For example, consider a linear single-degree-of-freedom system. In frequency domain, the response X is equal to the input F, magnified by the transfer function of the oscillator H:

$$X(\omega) = H(\omega)F(\omega) \tag{43}$$

Therefore, if the time-frequency model of the input is completely unknown, the output measurement does not have any saying on the transfer function of the oscillator since there exists a set of input to match with the measured output:

$$F(\omega) = X(\omega)/H(\omega) \tag{44}$$

In other words, identification of the model parameters is impossible in this case since all model parameters (as long as the associated transfer function is nonzero) give the same likelihood (perfect match) to the measurement.

However, if two or more DOFs are measured in a multistory building subjected to ground motion, the ratio between the responses of different DOFs will be constrained by the prescribed class of structural models, such as shear building models. In Ref. [118], a frequency-domain method for unknown input was proposed and it does not assume any time-frequency model for the input. The method takes the advantage that when the number of the measured channels is larger than the number of independent external excitations, there are mathematical constraints among the responses of different degrees of freedom. For example, when the building is subjected to earthquake ground motion, the number of independent input is one. If the responses of two or more degrees of freedom are measured for this building, there is information to infer the structural properties even though no assumption is made on the time-frequency content of the excitation. Specifically, the data is partitioned into two parts:

$$D^A = [\mathbf{y}_0^A, \mathbf{y}_1^A, \ldots, \mathbf{y}_{N-1}^A]; \quad D^B = [\mathbf{y}_0^B, \mathbf{y}_1^B, \ldots, \mathbf{y}_{N-1}^B] \tag{45}$$

where $\mathbf{y}_n^A$ and $\mathbf{y}_n^B$, $n = 0, 1, \ldots, N-1$, are the measurements corresponding to the first N_F and last $N_o - N_F$ DOFs, respectively. The number N_F denotes the dimension of the input $\mathbf{F}$. Then, the likelihood function can be expanded by the Bayes' theorem:

$$p(D|\boldsymbol{\theta},C) = p(D^A, D^B|\boldsymbol{\theta},C) = p(D^B|\boldsymbol{\theta},D^A,C)p(D^A|\boldsymbol{\theta},C) \tag{46}$$

It turns out that the likelihood function $p(D^A|\boldsymbol{\theta},C)$ does not depend on $\boldsymbol{\theta}$ for this partitioning arrangement and the conditional likelihood function $p(D^B|\boldsymbol{\theta},D^A,C)$ can be constructed in the frequency domain. The idea is that since the number of the independent excitation components is smaller than the number of observed degrees of freedom, one can develop easily the linear relationship between the Fourier transform of $\mathbf{Q}^A$ (measured quantity corresponding to $\mathbf{y}^A$) and $\mathbf{Q}^B$ (measured quantity corresponding to $\mathbf{y}^B$):

$$Q^B(\omega) = H^{BA}(\omega)Q^A(\omega) \tag{47}$$

where $Q^A(\omega)$ and $Q^B(\omega)$ are the discrete Fourier transform of the measured quantify $\mathbf{Q}^A$ and $\mathbf{Q}^B$; $H^{BA}(\omega)$ is the transfer function from $\mathbf{Q}^A$ to $\mathbf{Q}^B$ and it can be obtained easily using the excitation-response transfer function. For details, please refer to Ref. [118]. By using the relationship in Eq. (47), the likelihood function can be obtained by treating the measurement in D^A as the input:

$$p(D^A|\boldsymbol{\theta},D^B,C) = \kappa_7 \prod_{k\in \mathrm{K}} \frac{1}{(2\pi)^{(N_0-N_F)}\sqrt{|\Gamma(\omega_k)|}} \times \exp\left(-\frac{1}{2}\begin{bmatrix}\mathrm{Re}[\mathsf{Y}^B(\omega_k)]-\mu_R\\ \mathrm{Im}[\mathsf{Y}^B(\omega_k)]-\mu_I\end{bmatrix}^T \times \Gamma(\omega_k)^{-1}\begin{bmatrix}\mathrm{Re}[\mathsf{Y}^B(\omega_k)]-\mu_R\\ \mathrm{Im}[\mathsf{Y}^B(\omega_k)]-\mu_I\end{bmatrix}\right) \tag{48}$$

where μ_R and μ_I are the means and $\Gamma(\omega_k)$ is the covariance matrix and their expressions are given in Ref. [118]. However, caution must be made on the ill-posedness of the inverse problem since this relaxation of the assumption on the input stochastic model

Downloaded 29 Sep 2011 to 161.64.70.118. Redistribution subject to ASME license or copyright; see http://www.asme.org/terms/Terms_Use.cfm

breaks the bonding between different frequencies and induces a higher degree of ill conditioning of the problem. Therefore, the Bayesian framework is important to indicate if it is globally identifiable to avoid misleading results.

If the mathematical model for the concerned system has too many uncertain parameters, the measurement will not provide sufficient mathematical constraints/equations to uniquely identify the uncertain parameters. However, experienced engineers can identify the critical substructures for monitoring. Then, a free body diagram can be drawn to focus on these critical substructures only. Note that the internal forces on the boundary of the substructures are unknown and difficult to measure, so they are treated as uncertain input to the substructure [57,119]. Furthermore, these internal forces share the dominant frequencies of the structure so they cannot be modeled arbitrarily as white noise or other prescribed colored noise. However, with the same idea as in [118,120,121], these interface forces can be treated as unknown inputs without assuming their time-frequency content [122]. This enables a large number of possible applications in structural health monitoring and also enhances the computational efficiency since one does not need to consider the whole system.

5 Bayesian Model Updating Using Modal Measurements

This section introduces another type of Bayesian model updating techniques using modal measurements, i.e., modal frequencies and mode shapes. For structural/mechanical dynamics problems, the eigenvalues are the squared modal frequencies: $\lambda^{(m)} = \Omega^{(m)2}$, $m = 1, 2, \ldots, N_d$, and the eigenvectors, $\phi^{(1)}, \phi^{(2)}, \ldots, \phi^{(N_d)}$, are the mode shapes.

There are nonmodel based methods [123–129] and model based methods [130–134]. The method introduced here falls into the second category and most existing global structural health monitoring methods use dynamical model updating to determine local loss of stiffness by minimizing a measure of the difference between the modal frequencies and mode shapes measured in dynamic tests and those calculated from a finite-element model of the structure. The measured modal parameters are those estimated from dynamic test data using some modal identification procedure. A generic form of the goodness-of-fit function to be minimized is

$$J_g(\boldsymbol{\theta}) = \sum_{m=1}^{N_m} w_m [\lambda^{(m)}(\boldsymbol{\theta}) - \hat{\lambda}^{(m)}]^2 + \sum_{m=1}^{N_m} w'_m \left\| \phi^{(m)}(\boldsymbol{\theta}) - \hat{\phi}^{(m)} \right\|^2 \tag{49}$$

where $\hat{\lambda}^{(m)}$ and $\hat{\phi}^{(m)}$ are the measured eigenvalue and eigenvector of the mth mode; $\lambda^{(m)}(\boldsymbol{\theta})$ and $\phi^{(m)}(\boldsymbol{\theta})$ are the eigenvalue and eigenvector of the mth mode from the dynamical model with parameter vector $\boldsymbol{\theta}$ that determines the stiffness and mass matrix; and w_m and w'_m, $m = 1, 2, \ldots, N_m$, are chosen weightings that depend on the specific method. One major difficulty is that mode matching is required, i.e., it is necessary to determine which model mode matches which measured mode. If only measurements of partial mode shapes are available, this will not be a trivial task. Another major difficulty is that the N_m observed modes in dynamic tests might not necessarily be the N_m lowest-frequency modes in practice. In other words, some lower modes might not be detected. For example, some torsional modes are not excited. Furthermore, in the case where there is damage in the structure, the order of the modes might switch because the local loss of stiffness from damage may affect some modal frequencies more than others, making the mode matching even more challenging [135].

Recently, methods have been proposed for solving this model updating problem which avoid mode matching [136,137]. This is accomplished by employing the concept of system mode shapes that are used to represent the actual mode shapes of the structural system at all degrees of freedom corresponding to those of the dynamical model, but they are distinct from the mode shapes of the dynamical model, as will be seen more clearly later. Bayesian probabilistic methods are then used to update the dynamical model parameters and the system mode shapes based on the available modal data. Furthermore, Rayleigh quotient frequencies, which are based on the dynamical model and the system mode shapes, are employed instead of the modal frequencies of the dynamical model, so the eigenvalue problem needs never be solved.

As shown in previous research [136–138], the realistic assumption is made that only the modal frequencies and partial mode shapes of some modes are measured; system mode shapes are also introduced, which avoids mode matching between the measured modes and those of the dynamical model. The novel feature in this work is that system frequencies are also introduced as parameters to be identified in order to represent actual modal frequencies of the dynamical system (assuming that the dynamical behavior is well approximated by linear dynamics; otherwise they should be interpreted in the equivalent linear sense). The eigen equations of the dynamical model are used only in the prior probability distribution to provide soft constraints. Furthermore, to calculate the most probable values of the model parameters based on the modal data, an efficient iterative procedure is used that involves a series of coupled linear optimization problems, rather than directly solving the challenging nonlinear optimization problem by some general algorithms that may give convergence difficulties in the high-dimensional parameter space.

A class of dynamical models C is considered. It has a known mass matrix $\mathbf{M} \in R^{N_d \times N_d}$ (which is assumed to be established with sufficient accuracy from the engineering drawings of the structure) and the stiffness matrix $\mathbf{K} \in R^{N_d \times N_d}$ is parameterized by $\boldsymbol{\theta} = [\theta_1, \theta_2, \ldots, \theta_{N_\theta}]^T \in R^{N_\theta}$ as follows:

$$\mathbf{K}(\boldsymbol{\theta}) = \mathbf{K}_0 + \sum_{l=1}^{N_\theta} \theta_l \mathbf{K}_l \tag{50}$$

where the subsystem stiffness matrices $\mathbf{K}_l$, $l = 0, 1, \ldots, N_\theta$, are specified; e.g., by a finite-element model of the structure. The scaling parameters in $\boldsymbol{\theta}$ allow the nominal model matrix given by $\boldsymbol{\theta} = \boldsymbol{\theta}^\eta$ in Eq. (50) to be updated based on dynamic test data from the system.

Assume that N_m ($\leq N_d$) modes of the system are measured (not necessarily the first N_m lowest frequency modes), which have eigenvalues $\lambda^{(m)}$, $m = 1, 2, \ldots, N_m$, and real eigenvector components $\phi^{(m)} \in R^{N_d}$, $m = 1, 2, \ldots, N_m$. It is assumed that these modal parameters do not necessarily satisfy exactly the eigen equation with any given dynamical model $(\mathbf{M}, \mathbf{K}(\boldsymbol{\theta}))$ because there are always modeling approximations and errors. The quantities $\lambda^{(m)}$ and $\phi^{(m)}$ are referred to as the system eigenvalue and eigenvector of the mth mode to distinguish them from the corresponding modal parameters given by any dynamical model specified by $\boldsymbol{\theta}$. Given a parameter vector $\boldsymbol{\theta}$, the model can be defined in model class C. The prior probability density function for $\boldsymbol{\lambda} = [\lambda^{(1)}, \lambda^{(2)}, \ldots, \lambda^{(N_m)}]^T$ and $\Phi = [\phi^{(1)T}, \phi^{(2)T}, \ldots, \phi^{(N_m)T}]^T$ is chosen as

$$p(\boldsymbol{\lambda}, \Phi | \boldsymbol{\theta}, C) = \kappa_8 \exp\left[-\frac{1}{2} J_g(\boldsymbol{\lambda}, \Phi; \boldsymbol{\theta}) \right] \tag{51}$$

where κ_7 is a normalizing constant and the goodness-of-fit function is given by

$$J_g(\boldsymbol{\lambda}, \phi; \boldsymbol{\theta}) = \begin{bmatrix} (\mathbf{K}(\boldsymbol{\theta}) - \lambda^{(1)}\mathbf{M})\phi^{(1)} \\ (\mathbf{K}(\boldsymbol{\theta}) - \lambda^{(2)}\mathbf{M})\phi^{(2)} \\ \vdots \\ (\mathbf{K}(\boldsymbol{\theta}) - \lambda^{(N_m)}\mathbf{M})\phi^{(N_m)} \end{bmatrix}^T \Sigma_{eq}^{-1} \begin{bmatrix} (\mathbf{K}(\boldsymbol{\theta}) - \lambda^{(1)}\mathbf{M})\phi^{(1)} \\ (\mathbf{K}(\boldsymbol{\theta}) - \lambda^{(2)}\mathbf{M})\phi^{(2)} \\ \vdots \\ (\mathbf{K}(\boldsymbol{\theta}) - \lambda^{(N_m)}\mathbf{M})\phi^{(N_m)} \end{bmatrix} \tag{52}$$

The uncertainty in the equation errors for each mode are modeled as independent and identically distributed, so $\Sigma_{eq} = \sigma_{eq}^2 \mathbf{I}_{N_d N_m}$; σ_{eq}^2 is a prescribed equation-error variance. The usage of this variance

Downloaded 29 Sep 2011 to 161.64.70.118. Redistribution subject to ASME license or copyright; see http://www.asme.org/terms/Terms_Use.cfm

parameter allows for explicit treatment of modeling error as the parametric models for the stiffness matrix, and hence, the eigen equation, is never exact in practice. If this error level can be estimated, the mathematical constraint given by the eigen equation will become a soft constraint instead of a rigid constraint. In other words, errors of the eigen equation in the level corresponding to σ_{eq} is allowed. The value of σ_{eq}^2 may be chosen to be very small so that the eigen equations are nearly satisfied. This means that the system modal frequencies and mode shapes will correspond closely to modal parameters of the identified dynamical model. For modal data from a real structure, this would be a reasonable strategy to start with. If the measured modal parameters did not agree well with those corresponding to the identified (most probable) dynamical model, implying considerable modeling errors, then σ_{eq}^2 could be increased. This procedure allows explicit control of the inherent trade-off between how well the measured modal parameters are matched and how well the eigen equations of the identified dynamical model are satisfied. This additional modeling flexibility is an appealing feature of this method.

The prior PDF $p(\boldsymbol{\lambda}, \Phi|\boldsymbol{\theta}, C)$ implies that, given a class of dynamical models and before using the dynamic test data, the most probable values of $\boldsymbol{\lambda}$ and Φ are those that minimize the Euclidean norm (2-norm) of the error in the eigen equation for the dynamical model. This implies that the prior most probable values of $\boldsymbol{\lambda}$ and Φ are the squared modal frequencies and mode shapes of a dynamical model, but these values are never explicitly required. This prior PDF will have multiple peaks because there is no implied ordering of the modes here.

The prior PDF for all the unknown parameters is given by

$$p(\boldsymbol{\lambda}, \Phi, \boldsymbol{\theta}|C) = p(\boldsymbol{\lambda}, \Phi|\boldsymbol{\theta}, C)p(\boldsymbol{\theta}|C) \tag{53}$$

where the prior PDF $p(\boldsymbol{\theta}|C)$ can be taken as a Gaussian distribution with mean $\boldsymbol{\theta}^\eta$ representing the nominal values of the model parameters and with covariance matrix $\Sigma_{\boldsymbol{\theta}}$. For example, the prior covariance matrix $\Sigma_{\boldsymbol{\theta}}$ can be taken as diagonal with large variances, giving virtually a noninformative prior.

To construct the likelihood function, the measurement error $\boldsymbol{\varepsilon}$ is introduced:

$$\begin{bmatrix} \hat{\boldsymbol{\lambda}} \\ \hat{\Psi} \end{bmatrix} = \begin{bmatrix} \boldsymbol{\lambda} \\ \mathbf{L}_o \Phi \end{bmatrix} + \boldsymbol{\varepsilon} \tag{54}$$

and a Gaussian probability model is chosen for $\boldsymbol{\varepsilon} \in R^{N_m(N_o+1)}$ with zero mean and covariance matrix Σ_ε, which can be obtained by Bayesian modal identification methods (such as the ones introduced in the previous sections); $\hat{\Psi} = [\hat{\varphi}^{(1)T}, \hat{\varphi}^{(2)T}, \ldots, \hat{\varphi}^{(N_m)T}]^T$ and $\hat{\boldsymbol{\lambda}} = [\hat{\lambda}^{(1)}, \hat{\lambda}^{(2)}, \ldots, \hat{\lambda}^{(N_m)}]^T$, where $\hat{\varphi}^{(m)} \in R^{N_o}$ gives the observed components of the system eigenvector of the mth mode and $\hat{\lambda}^{(m)}$ gives the corresponding observed system eigenvalue from dynamic test data. Finally, $\mathbf{L}_o$ is an $N_m N_o \times N_d N_m$ observation matrix of 1's or 0's that picks the components of Φ corresponding to the N_o measured degrees of freedom. The likelihood function is therefore

$$p(\hat{\boldsymbol{\lambda}}, \hat{\Psi}|\boldsymbol{\lambda}, \Phi, \boldsymbol{\theta}, C) = p(\hat{\boldsymbol{\lambda}}, \hat{\Psi}|\boldsymbol{\lambda}, \Phi) \tag{55}$$

is a Gaussian distribution with mean $[\boldsymbol{\lambda}^T, (\mathbf{L}_o\Phi)^T]^T$ and covariance matrix Σ_ε.

The posterior PDF for the unknown parameters is given by the Bayes' theorem:

$$\begin{aligned} p(\boldsymbol{\lambda}, \Phi, \boldsymbol{\theta}|\hat{\boldsymbol{\lambda}}, \hat{\Psi}, C) &= \kappa_9 p(\hat{\boldsymbol{\lambda}}, \hat{\Psi}|\boldsymbol{\lambda}, \Phi, \boldsymbol{\theta}, C)p(\boldsymbol{\lambda}, \Phi|\boldsymbol{\theta}, C)p(\boldsymbol{\theta}|C) \\ &= \kappa_9 p(\hat{\boldsymbol{\lambda}}, \hat{\Psi}|\boldsymbol{\lambda}, \Phi)p(\boldsymbol{\lambda}, \Phi|\boldsymbol{\theta}, C)p(\boldsymbol{\theta}|C) \end{aligned} \tag{56}$$

The most probable values of the unknown parameters can be found by maximizing this PDF. To proceed, the objective function is defined as Ref. [139]:

$$\begin{aligned} J(\boldsymbol{\lambda}, \Phi, \boldsymbol{\theta}) = &\frac{1}{2}(\boldsymbol{\theta} - \boldsymbol{\theta}^\eta)^T \Sigma_\theta^{-1} (\boldsymbol{\theta} - \boldsymbol{\theta}^\eta) \\ &+ \frac{1}{2\sigma_{eq}^2} \sum_{m=1}^{N_m} \|(\mathbf{K}(\boldsymbol{\theta}) - \lambda^{(m)}\mathbf{M})\phi^{(m)}\|^2 \\ &+ \frac{1}{2} \begin{bmatrix} \hat{\boldsymbol{\lambda}} - \boldsymbol{\lambda} \\ \hat{\Psi} - \mathbf{L}_o\Phi \end{bmatrix}^T \Sigma_\varepsilon^{-1} \begin{bmatrix} \hat{\boldsymbol{\lambda}} - \boldsymbol{\lambda} \\ \hat{\Psi} - \mathbf{L}_o\Phi \end{bmatrix} \end{aligned} \tag{57}$$

which is the negative logarithm of the posterior PDF without including the constant that does not depend on the uncertain parameters. Here, $||.||$ denotes the Euclidean norm. Then, the function $J(\boldsymbol{\lambda}, \Phi, \boldsymbol{\theta})$ is minimized instead of maximizing the posterior PDF. This objective function is not quadratic for the uncertain parameters. However, this function is quadratic for any of the uncertain parameter vector of $\boldsymbol{\lambda}$, Φ or $\boldsymbol{\theta}$ if the other two are fixed. Therefore, the original nonlinear optimization problems can be done iteratively through a sequence of linear optimization problems.

The mode shapes are usually measured/identified with incomplete components, i.e., with missing DOFs but the modal frequencies are measured with relatively high accuracy. Therefore, the sequence of optimization starts from computing the missing components of the mode shapes. First set the updated model parameters at their nominal values ($\boldsymbol{\theta}^* = \boldsymbol{\theta}^\eta$) and the eigenvalues at their measured values ($\boldsymbol{\lambda}^* = \hat{\boldsymbol{\lambda}}$). Then, perform a sequence of iterations comprised of the following linear optimization problems:

$$\Phi^* = \arg\min_{\Phi} J(\boldsymbol{\lambda}^*, \Phi, \boldsymbol{\theta}^*); \quad \boldsymbol{\lambda}^* = \arg\min_{\boldsymbol{\lambda}} J(\boldsymbol{\lambda}, \Phi^*, \boldsymbol{\theta}^*);$$
$$\boldsymbol{\theta}^* = \arg\min_{\boldsymbol{\theta}} J(\boldsymbol{\lambda}^*, \Phi^*, \boldsymbol{\theta})$$

until the prescribed convergence criteria is satisfied and these three optimization problems is explained in more detail in the following.

By minimizing the objective function $J(\boldsymbol{\lambda}, \Phi, \boldsymbol{\theta})$ in Eq. (57) with respect to Φ, the optimal vector Φ^* can be obtained:

$$\Phi^* = \left[\sigma_{eq}^{-2} \begin{bmatrix} (\lambda^{(1)*}\mathbf{M} - \mathbf{K}^*)^2 & & \mathbf{0} \\ & \ddots & \\ \mathbf{0} & & (\lambda^{(N_m)*}\mathbf{M} - \mathbf{K}^*)^2 \end{bmatrix} + \mathbf{L}_o^T \left(\Sigma_\varepsilon^{-1}\right)_{22} \mathbf{L}_o \right]^{-1} \times \mathbf{L}_o^T \left[\left(\Sigma_\varepsilon^{-1}\right)_{21} \left(\hat{\boldsymbol{\lambda}} - \boldsymbol{\lambda}^*\right) + \left(\Sigma_\varepsilon^{-1}\right)_{22} \hat{\Psi} \right] \tag{58}$$

where $\left(\Sigma_\varepsilon^{-1}\right)_{21}$ and $\left(\Sigma_\varepsilon^{-1}\right)_{22}$ are the $N_m N_o \times N_m$ left bottom and $N_m N_o \times N_m N_o$ right bottom sub-matrices of Σ_ε^{-1}; and the updated stiffness matrix $\mathbf{K}^* = \mathbf{K}(\boldsymbol{\theta}^*)$.

By minimizing the objective function $J(\boldsymbol{\lambda}, \Phi, \boldsymbol{\theta})$ in Eq. (57) with respect to $\boldsymbol{\lambda}$, the updated parameter vector $\boldsymbol{\lambda}^*$ is given by

Downloaded 29 Sep 2011 to 161.64.70.118. Redistribution subject to ASME license or copyright; see http://www.asme.org/terms/Terms_Use.cfm

$$\boldsymbol{\lambda}^* = \left[\begin{bmatrix} \phi^{(1)*T}\mathbf{M}^2\phi^{(1)*} & & \mathbf{0} \\ & \ddots & \\ \mathbf{0} & & \phi^{(N_m)*T}\mathbf{M}^2\phi^{(N_m)*} \end{bmatrix} + \left(\Sigma_\varepsilon^{-1}\right)_{11} \right]^{-1} \times \left(\sigma_{eq}^{-2} \begin{bmatrix} \phi^{(1)*T}\mathbf{M}\mathbf{K}^*\phi^{(1)*} \\ \phi^{(2)*T}\mathbf{M}\mathbf{K}^*\phi^{(2)*} \\ \vdots \\ \phi^{(N_m)*T}\mathbf{M}\mathbf{K}^*\phi^{(N_m)*} \end{bmatrix} + \left(\Sigma_\varepsilon^{-1}\right)_{11}\hat{\boldsymbol{\lambda}} + \left(\Sigma_\varepsilon^{-1}\right)_{12}\left(\hat{\Psi} - \mathbf{L}_o\phi^*\right) \right) \tag{59}$$

where $\left(\Sigma_\varepsilon^{-1}\right)_{11}$ and $\left(\Sigma_\varepsilon^{-1}\right)_{12}$ are the $N_m \times N_m$ left top and $N_m \times N_m N_o$ right top sub-matrices of Σ_ε^{-1}.

By minimizing Eq. (57) with respect to $\boldsymbol{\theta}$, the updated model parameter vector $\boldsymbol{\theta}^*$ is given by

$$\boldsymbol{\theta}^* = \left(\sigma_{eq}^{-2}\mathbf{G}_\theta^T\mathbf{G}_\theta + \Sigma_\theta^{-1}\right)^{-1} \times \left(\sigma_{eq}^{-2}\mathbf{G}_\theta^T \begin{bmatrix} (\lambda^{(1)*}\mathbf{M} - \mathbf{K}_0)\phi^{(1)*} \\ \vdots \\ (\lambda^{(N_m)*}\mathbf{M} - \mathbf{K}_0)\phi^{(N_m)*} \end{bmatrix} + \Sigma_\theta^{-1}\boldsymbol{\theta}^\eta \right) \tag{60}$$

where the matrix $\mathbf{G}_\theta$ is given by

$$\mathbf{G}_\theta = \begin{bmatrix} \mathbf{K}_1\phi^{(1)*} & \mathbf{K}_2\phi^{(1)*} & \cdots & \mathbf{K}_{N_\theta}\phi^{(1)*} \\ \mathbf{K}_1\phi^{(2)*} & \mathbf{K}_2\phi^{(2)*} & \cdots & \mathbf{K}_{N_\theta}\phi^{(2)*} \\ \vdots & \vdots & \ddots & \vdots \\ \mathbf{K}_1\phi^{(N_m)*} & \mathbf{K}_2\phi^{(N_m)*} & \cdots & \mathbf{K}_{N_\theta}\phi^{(N_m)*} \end{bmatrix}_{N_d N_m \times N_\theta} \tag{61}$$

The iterative procedure consists of the following steps:

(1) Take the initial values of the model parameters as the nominal values: $\boldsymbol{\theta}^* = \boldsymbol{\theta}^\eta$, and the eigenvalues as the measured values: $\boldsymbol{\lambda}^* = \hat{\boldsymbol{\lambda}}$. Then, $\mathbf{K}^* = \mathbf{K}(\boldsymbol{\theta}^*)$.
(2) Update the estimates of the system eigenvectors $\phi^{(m)*}$, $m = 1, 2, \ldots, N_m$, using Eq. (58).
(3) Update the estimates of the system eigenvalues (squared modal frequencies) $\lambda^{(m)*}$, $m = 1, 2, \ldots, N_m$, using Eq. (59).
(4) Update the estimates of the model parameters $\boldsymbol{\theta}^*$ by using Eq. (60)
(5) Iterate Steps 2, 3 and 4 until the model parameters in $\boldsymbol{\theta}^*$ satisfy some convergence criterion, thereby giving the most probable values of the model parameters based on the modal data.

The posterior PDF in Eq. (56) can be well approximated by a Gaussian distribution centered at the optimal (most probable) parameters $(\boldsymbol{\lambda}^*, \Phi^*, \boldsymbol{\theta}^*)$ and with covariance matrix $\Sigma(\boldsymbol{\lambda}, \Phi, \boldsymbol{\theta})$ equal to the inverse of the Hessian of the objective function $J(\boldsymbol{\lambda}, \Phi, \boldsymbol{\theta}) = -\ln p(\boldsymbol{\lambda}, \Phi, \boldsymbol{\theta}|\hat{\boldsymbol{\lambda}}, \hat{\Psi}, C)$ calculated at the optimal parameters. For details, the expression can be found in Ref. [87].

6 Model Complexity, Sensitivity, Data Fitting Capability and Robustness

This section discusses the relationship among complexity, output sensitivity, data capability and robustness of identification model class. This is a very important issue because it plays a major role on the quality of identification results. Influenced by the mind of forward modeling, it is easily directed to adopt complicated model classes in order to capture various physical behavior/mechanism. However, the more complex the model class, the more uncertain parameters are usually introduced unless extra mathematical constraints of these parameters are imposed. In the former case, the model output may not necessarily be accurate even if the model well characterizes the underlying phenomenon/system since the combination of the many small errors from each uncertain parameter can induce large output error. Furthermore, it may lead to an unidentifiable model so the uncertain parameters cannot be uniquely determined. In the latter case, it is inevitable that the extra constraints/approximations induce substantial errors. Therefore, it is important to use a proper model class for parametric identification purpose. For example, consider a detailed identification model with thousands of degrees of freedom for a highrise building. For such a model, there will be a large number of structural elements (beams, columns, plates, …) associated with uncertain mass and stiffness parameters. It is obvious that the model is unidentifiable unless a huge number of sensors are used to give sufficient constraints to the identification problem. One way to resolve the identifiability problem is to enforce extra constraints so as to reduce the number of uncertain parameters, e.g., by assuming rigid floor or grouping the stiffness parameters with a prescribed proportion. However, such simplification/approximation will induce modeling error to the identification model.

It is clear that a suitable model class for identification should be capable to fit the data well and to provide sufficient robustness to modeling error and measurement noise [140]. Now, an example is used to illustrate that there is no definite relationship between posterior uncertainty and data fitting capability. Consider an example of two single-parameter model classes with likelihood functions satisfying the following relationship for the same set of measurement: $p(D|\theta_1 = \theta, C_1) = 2p(D|\theta_2 = \theta, C_2)$ so $\ln p(D|\theta_1 = \theta, C_1) = \ln p(D|\theta_2 = \theta, C_2) + \ln 2$. Here, D denotes the measurement; θ_1 and θ_2 are the uncertain parameter for model class C_1 and C_2, respectively. With the same prior distribution, the posterior distributions and uncertainty of the parameters in these two model classes are identical since the difference between the log-likelihood functions is a constant (Eq. (14)). However, model class C_1 fits the data better as its maximum likelihood value is twice of that for C_2: $p(D|\theta_1^*, C_1) = 2p(D|\theta_2^*, C_2)$, where θ_1^* and θ_2^* are the optimal parameters for the two model classes. Therefore, the same level of posterior uncertainty is associated with different levels of data fitting in this case. This example demonstrates that the degree of data fitting has no direct relationship with the posterior uncertainty of the parameters.

Posterior uncertainty is a measure of the spread of the posterior distribution, which is proportional to the product of the prior distribution and the likelihood function. According to Ref. [87], small posterior uncertainty is possible to associate with poor data fitting. On the other hand, sensitivity can be defined as the change of the model output due to unit parameter perturbation. The slope of the posterior PDF depends on the sensitivity, which controls the rate of the change of the model output due to perturbation of the parameters. On the other hand, posterior uncertainty of the parameters is controlled by the decaying rate (slope) of the posterior PDF in the neighborhood around the optimal point. Therefore, it is particularly important to investigate the sensitivity of a model around the optimal parameters. If a model class is utilized for future prediction, it is desirable to obtain a robust model class that fits the data well even with error in the parameters. In this case, the maximum likelihood value has to be large and the likelihood value remains large in a sufficiently large region. In other words, the topology of the likelihood function around the maximum is reasonably flat (i.e., the output sensitivity is low).

Figure 1 shows schematically two likelihood functions to demonstrate this relationship. The two likelihood functions are assumed to be obtained with the same set of measurement but with different model classes. Model class C_1 obviously has larger

Downloaded 29 Sep 2011 to 161.64.70.118. Redistribution subject to ASME license or copyright; see http://www.asme.org/terms/Terms_Use.cfm

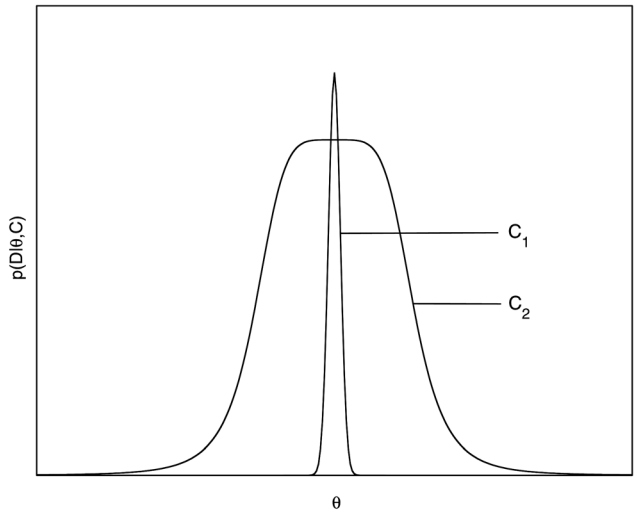

Fig. 1 Schematic plot of two likelihood functions

maximum likelihood value than C_2, indicating that the optimal model in C_1 fits the data better than that of C_2. Furthermore, the posterior uncertainty of the parameter in C_1 is smaller than that of C_2 if the same prior distribution is used. However, if the optimal models are used for future prediction, model class C_2 is more reliable since it has a larger parameter range that provides satisfactory fitting to the data. Therefore, mode class C_2 is more robust. On the other hand, the maximum likelihood margin of C_1 may be insufficient to compensate if the model parameter has tiny error. Therefore, a reliable model class should have reasonable balance between data fitting capability and robustness to modeling error. This example also demonstrates that even for the same number of parameters, a model class with larger maximum likelihood value is not necessarily more suitable for parametric identification.

Table 1 shows the four combinations of data fitting capability and posterior uncertainty. It is desirable to use a model class with high maximum likelihood value and large posterior uncertainty so that efficient and robust identification performance can be expected. However, this is difficult to achieve. Although data fitting capability can be enhanced by adding free parameters, this will inevitably degrade the robustness of a model class. Therefore, a suitable model class should possess reasonable balance between these two properties. It should be noted that the complexity of a model class depends not only on the number of its adjustable parameters but also the specific structure of the solution space.

One possible way to rank among prescribed model classes is the Bayesian model class selection approach, which utilizes the measurement, D, from the underlying system. Since probability may be interpreted as a measure of plausibility based on specified information [141], the posterior plausibility of a model class C_j is given by [142–144]:

$$P(C_j|D) = \frac{p(D|C_j)P(C_j)}{\sum_{j=1}^{N_C} p(D|C_j)P(C_j)}, \quad j = 1, 2, \ldots, N_C \tag{62}$$

where $p(D|C_j)$ is the evidence for model class C_j, $P(C_j)$ is the prior plausibility of C_j and the denominator is a normalizing constant such that the total posterior plausibility is normalized to be unity: $\sum_{j=1}^{N_C} P(C_j|D) = 1$. In most applications, uniform prior plausibility can be taken so the model class selection will rely solely on the measurement, i.e., $P(C_j) = 1/N_C, j = 1, \ldots, N_C$.

Table 1 Likelihood, posterior uncertainty and robustness

Maximum likelihood value	High	Low
Large posterior uncertainty	Efficient and robust	Poor modeling
Small posterior uncertainty	Efficient but fragile	Poor modeling

Use $\boldsymbol{\theta}_j \in \mathrm{R}^{N_j}$ to denote the uncertain parameter vector in the parameter space Θ_j for model class C_j, where N_j is the number of uncertain parameters. By the theorem of total probability, the evidence of C_j is given by:

$$p(D|C_j) = \int_{\Theta_j} p(D|\boldsymbol{\theta}_j, C_j)p(\boldsymbol{\theta}_j|C_j)d\boldsymbol{\theta}_j \tag{63}$$

where $p(D|\boldsymbol{\theta}_j, C_j)$ is the likelihood function of model class C_j and $p(\boldsymbol{\theta}_j|C_j)$ is the prior distribution of the uncertain parameters. For a large number of data points, the integrand in the evidence integral in Eq. (63) can be well approximated as an unnormalized Gaussian distribution so this evidence integral can be approximated by the Laplace's asymptotic approximation [145]:

$$p(D|C_j) \approx p(D|\boldsymbol{\theta}_j^*, C_j)F_j \tag{64}$$

where $p(D|\boldsymbol{\theta}_j, C_j)$ is the likelihood function of model class C_j and $p(\boldsymbol{\theta}_j|C_j)$ is the prior distribution of the uncertain parameters; $\boldsymbol{\theta}_j^*$ is the optimal parameter vector that maximizes the integrand in Eq. (63) and the Ockham factor F_j represents the penalty against complicated parameterization [143,146]:

$$F_j \equiv p(\boldsymbol{\theta}_j^*|C_j)(2\pi)^{N_j/2}|\mathbf{H}_j(\boldsymbol{\theta}_j^*)|^{-1/2} \tag{65}$$

The matrix $\mathbf{H}_j(\boldsymbol{\theta}_j^*)$ is the Hessian matrix of objective function $-\ln[p(D|\boldsymbol{\theta}_j, C_j)p(\boldsymbol{\theta}_j|C_j)]$ evaluated at $\boldsymbol{\theta}_j = \boldsymbol{\theta}_j^*$. By Eq. (64), the evidence of a model class represents the competition between data fitting capability (measured by the maximum likelihood value $p(D|\boldsymbol{\theta}_j^*, C_j)$) and the robustness of the model class (measured by the Ockham factor). Hence, the most plausible model class is the one that possesses the best trade-off between the data fitting efficiency and robustness to modeling error. This approach has been applied to a number of engineering problems, including architecture of neural networks [105,147], damage detection [148], estimation of fault rupture extent [149]; identification for hysteretic structural dynamical models [150], air quality modeling [151], soil compressibility relationship [152], biomedical engineering [153], environmental effects to structural modal parameters [154], structural integrity monitoring [155], crack detection [156,157], and seismic attenuation relationship [158]. For more general cases in which the Gaussian approximation is inappropriate, one may use the transitional Markov chain Monte Carlo simulation method [159] to evaluate directly the evidence integral in Eq. (63).

Next, we examine the Bayesian model class selection approach accordingly. By Eq. (63), it is clear that the evidence integral is the standard inner product of the prior distribution and the likelihood function. In order to possess a high value of the evidence, a good model class should have large likelihood value over a reasonably large region, which overlaps with the significant region of the prior distribution. Furthermore, the prior distribution values are important even if a uniform distribution is used and this is in contrast to parametric identification. In parametric identification, noninformative prior distribution is often used to let the identification rely solely on the likelihood of the data. As long as it is sufficiently flat and covers the significant region of the likelihood function, the identification results will virtually be independent to the choice of the prior distribution. Therefore, it is popular to even absorb the prior distribution into the normalizing constant to obtain the maximum likelihood solution. However, this is not the case for model class selection. For example, doubling the range of a sufficiently wide uniform prior distribution will reduce its probability density value by half. This will not affect the parametric identification results but the evidence will be half. If the user has a lot of experience of a particular model class, the prior information allows the use of a more concentrated prior distribution of the uncertain parameters. This leads to a larger value of the evidence

Downloaded 29 Sep 2011 to 161.64.70.118. Redistribution subject to ASME license or copyright; see http://www.asme.org/terms/Terms_Use.cfm

if the region with significant prior distribution values overlaps with that of the likelihood function. On the other hand, this approach does not penalize an unidentifiable model class. Finally, by examining the example in Fig. 1 again, model class C_2 is preferred by the Bayesian model class selection approach if the same prior distribution is used for the parameters of both model classes. It confirms that the Bayesian approach selects the model class with good data fitting capability and yet with sufficient robustness.

7 Illustration Example: Structural Response of a Building Under Severe Typhoon

This example utilizes the response measurement of a 22-story building, namely the East Asia Hall. It was inaugurated in 2005 for lodging athletes during the 4th East Asian Games hosted in Macao. Since then, it has been serving as a dormitory of University of Macau. It is a reinforced concrete building of 64.70 m height, and its floor layer is in L-shape with unequal spans of 51.90 m and 61.75 m. A typical floor plan is shown in Fig. 2. In contrast to most of the monitored buildings with regular configurations (such as rectangular or circular floor layer) and large height-to-width aspect ratios [160–163], the East Asia Hall has an L-shape floor section with aspect ratio close to unity. Due to the particular geometry of the building, the aerodynamic effect to the structural behavior is significantly more complex [164,165]. In this study, its response measurement under a severe typhoon, namely Hagupit, is analyzed.

On Sept. 14, 2008, a tropical disturbance was formed to the northeast of Guam and moved towards the Philippines. Being gradually intensified in the following days, the disturbance became a tropical storm and it was named Hagupit on Sept. 19. On the same day, it was upgraded to a tropical storm and it was approaching southern China. The track of Hagupit is shown in Fig. 3. Hagupit was dissipated after the landfall was made between the Guangdong and Guangxi province on Sept. 24. Afterwards, the typhoon signal was cancelled at 16:00 on the same day. Hagupit had the highest ten-minute sustained wind speed of 165 km/hr and the lowest pressure of 935 hPa. More than 60 people were killed and the economic loss was estimated to be no less than 1×10^9 US dollars. Hagupit was the strongest typhoon affected Macao since year 2000 and it generated the most severe wind loading on the East Asian Hall in the history of the building.

Figure 4 shows the wind speed and wind direction observed at the Meteorological and Geophysical Bureau of Macao. One can observe that between the 20th to 35th hour, the wind direction rotated gradually from north to east and then to south. When a typhoon is approaching, the wind speed increases gradually while the wind direction changes. Once it reaches the closest point to a city, the wind speed achieves the highest magnitude. Meanwhile, the wind direction will change drastically if the typhoon is very close. Therefore, the wind loading generated by a typhoon, and

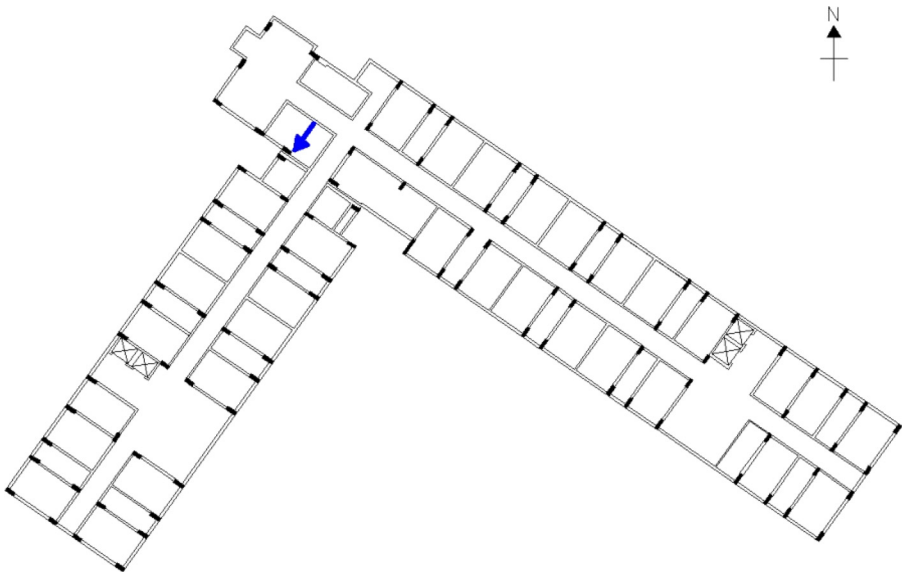

Fig. 2 A typical floor plan of the East Asia Hall

Fig. 3 Track of Hagupit (provided by the Meteorological and Geophysical Bureau (http://www.smg.gov.mo/c_index.php) and the time corresponds to GMT +08:00)

Downloaded 29 Sep 2011 to 161.64.70.118. Redistribution subject to ASME license or copyright; see http://www.asme.org/terms/Terms_Use.cfm

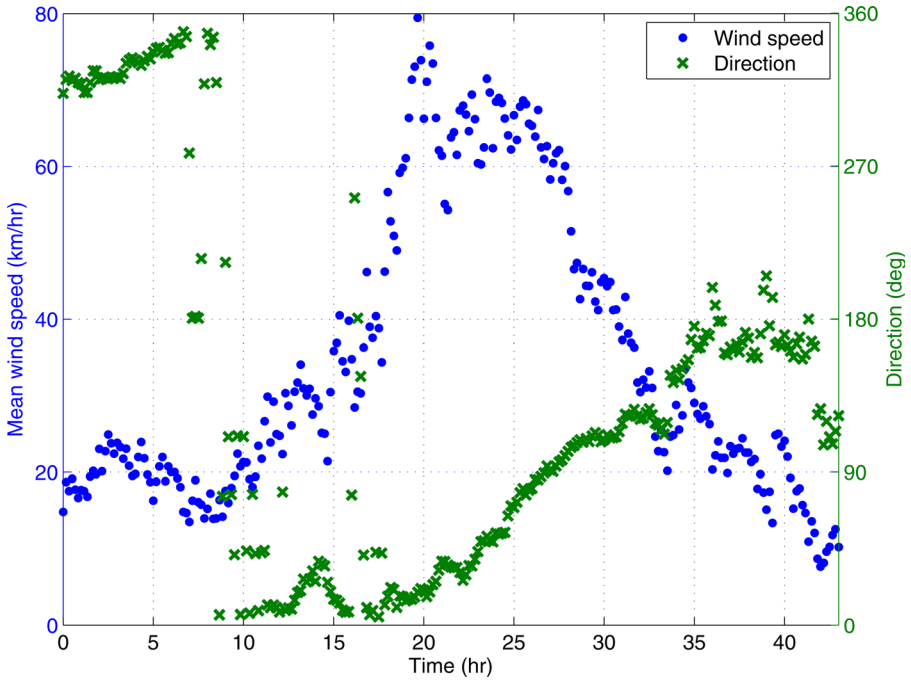

Fig. 4 Wind speed and wind direction

hence the structural response, is considered as a nonstationary stochastic process, especially when the typhoon is close to the city [166,167]. As shown on the right tails of the figure, the typhoon-effect was mitigated after the landfall was made and the major wind direction was recovered to the background prevalent offshore wind direction.

Acceleration time histories of the East Asia Hall were recorded on the 18th story and its direction is shown in Fig. 2. The duration of the measurement was 43hs which covered the whole duration of Hagupit, with sampling frequency 500 Hz. Fig. 5 shows the root-mean-square acceleration and the ten minute-average wind speed observed in Macao by the Meteorological and Geophysical Bureau of the Macao government. The rectangular window encloses the region in which the wind speed exceeded 40 km/hr and the two arrows indicate the peaks of the wind speed and structural response. It is observed that the structural acceleration magnitude on the right boundary of the high-wind-speed window was about twice of the left boundary, but they are associated with the same wind speed (40 km/hr). Moreover, the arrows indicate that the peaks of the RMS acceleration and wind speed did not occur at the same time. This is caused by the wind attacking angle of the typhoon. From Fig. 4, the wind direction changed gradually from north to east and the drag coefficient was increasing in this process. Under the same wind speed, larger resultant force was created in the later stage so the corresponding structural response was larger. It turned out that the peak of the structural response occurred 7 hs after the peak of the wind speed. When the maximum response was achieved, the wind speed was 20% lower than its maximum value.

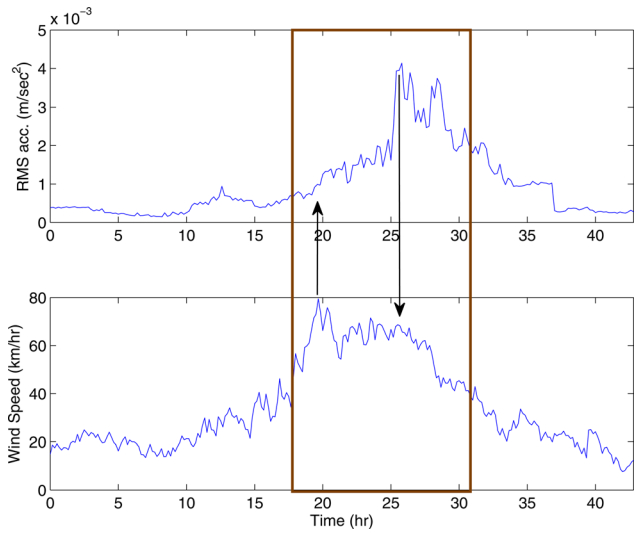

Fig. 5 RMS acceleration and mean wind speed

In the present study, the modal parameters of the structure and the excitation are identified using the Bayesian spectral density approach for each of the five-minute records in order to trace their fluctuation. The spectral density estimators are used up to 1.6 Hz, which is roughly the middle of the first two peaks in the spectrum. Figure 6 shows the identification results and there are three curves. The middle one shows the identified modal frequency using each of the five-minute acceleration record. The identified modal frequency is referred to the equivalent modal frequency since the building may not behave perfectly linear, especially under the severe wind pressure. The intervals between the other two curves are the confidence intervals with probability 99%. It is statistically evident that there was notable reduction of the modal frequency in the high wind speed region and the maximum estimated reduction was 6%. Note that this can be concluded because the uncertainty of the identified values can be quantified using the Bayesian method. Such reduction was recovered almost immediately after the typhoon was dissipated and the ambient conditions (temperature and humidity) went back to normal situation [168].

The Bayesian fast Fourier transfer approach is also applied to the same set of measurements. It is not surprising that the results, including the identified values and the uncertainty estimates, are virtually the same as those by the Bayesian spectral density approach. It is because these two frequency-domain methods utilize the same approximation of independency in the same frequency range. The only difference is that the Bayesian fast Fourier transform approach considers the exact covariance matrices of the fast Fourier transforms while the Bayesian spectral density approach further approximates the structure of these matrices

Downloaded 29 Sep 2011 to 161.64.70.118. Redistribution subject to ASME license or copyright; see http://www.asme.org/terms/Terms_Use.cfm

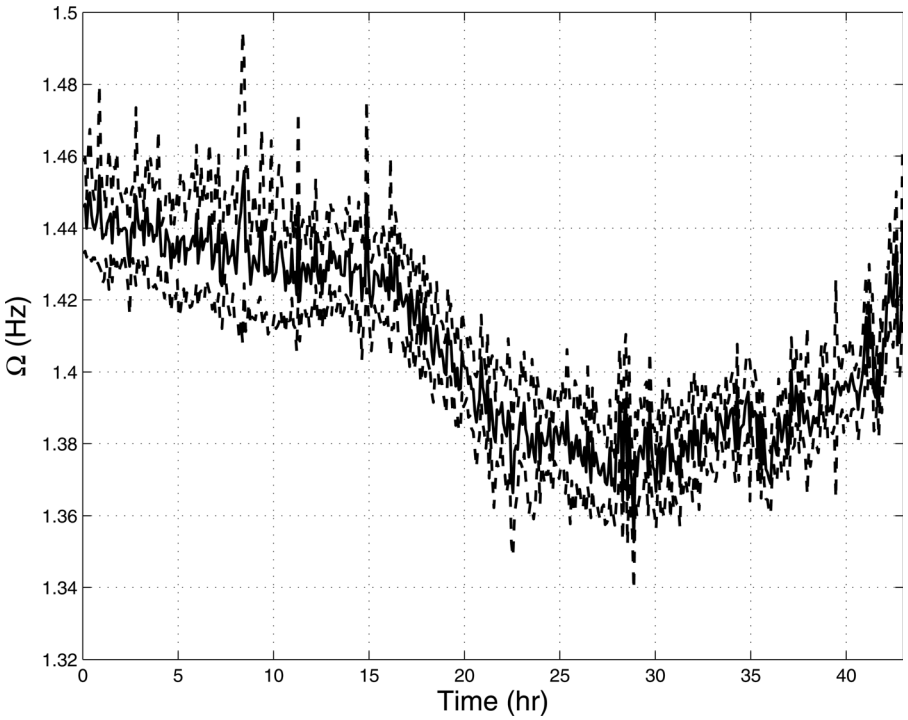

Fig. 6 Identified values of the modal frequency using Bayesian spectral density approach

to obtain the Wishart distribution. However, this approximation is sufficiently accurate, especially in the frequency range considered, so the results are practically the same. On the other hand, it should be noted that the computational effort required by the Bayesian fast Fourier transform approach is significantly higher than the Bayesian spectral density approach because the size of the matrices and vectors involved in the former is twice of the latter.

Furthermore, the Bayesian time-domain approach is also applied to analyze the same set of measurements. As in the Bayesian spectral density approach, the measurement is used up to 1.6 Hz and the response in each five-minute time intervals is assumed stationary. The truncation variable N_p in Eq. (19) is taken as 50 so that the conditioning data points cover slightly more than one fundamental period of this structure. Figure 7 shows the identified

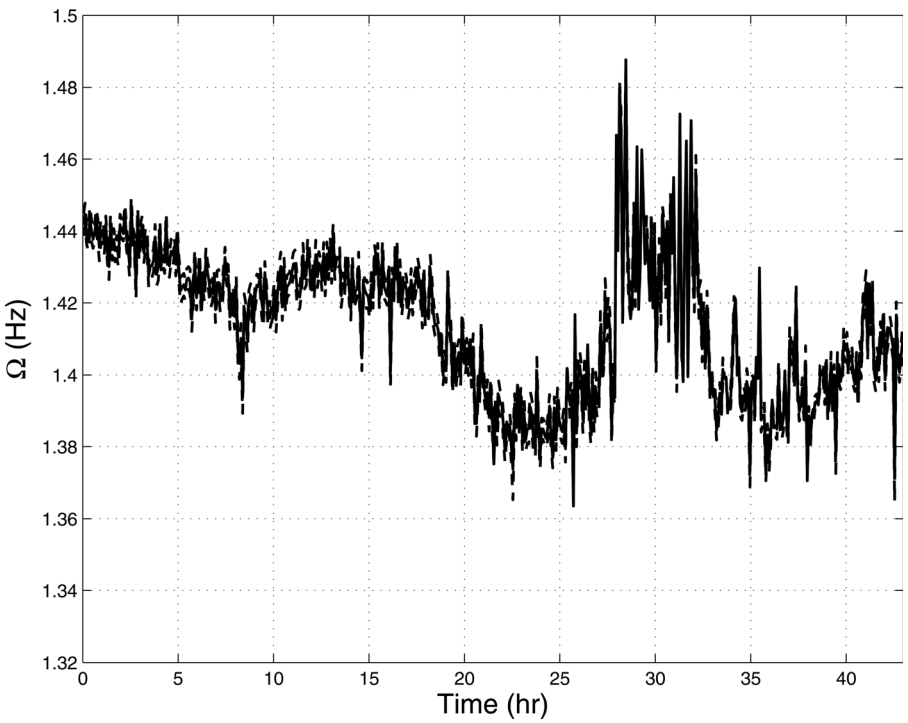

Fig. 7 Identified values of the modal frequency using Bayesian time-domain approach

Downloaded 29 Sep 2011 to 161.64.70.118. Redistribution subject to ASME license or copyright; see http://www.asme.org/terms/Terms_Use.cfm

modal frequencies and the associated confidence intervals in the same way as Fig. 6. It turns out that there are some discrepancies of the identified values from the 28th to 32nd hour between the time-domain and frequency-domain approaches. It is believed that the results obtained by the latter are more reliable as these frequency-domain methods are more robust to modeling error, such as linearity of structures, probability distribution of the input and measurement noise, stationarity of the response, etc. Moreover, the identified values by the Bayesian time-domain approach are substantially more fluctuating in consecutive five-minute intervals during the aforementioned five hours. On the other hand, the confidence intervals obtained by the Bayesian time-domain approach are significantly narrower than the frequency-domain approaches because the former utilizes all information of the data while the frequency-domain approaches use only a much narrower frequency band. However, one should note that these uncertainty estimates do not take into account the bias induced by the violation of assumptions and this will be an important subject for further study.

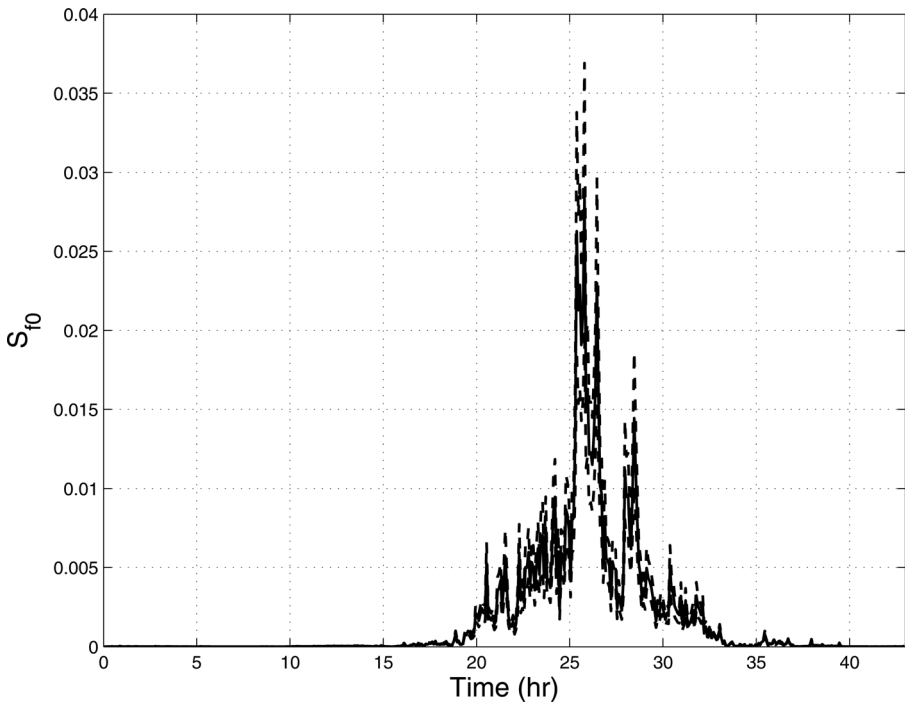

Fig. 8 Identified values of the modal spectral intensity using Bayesian spectral density approach

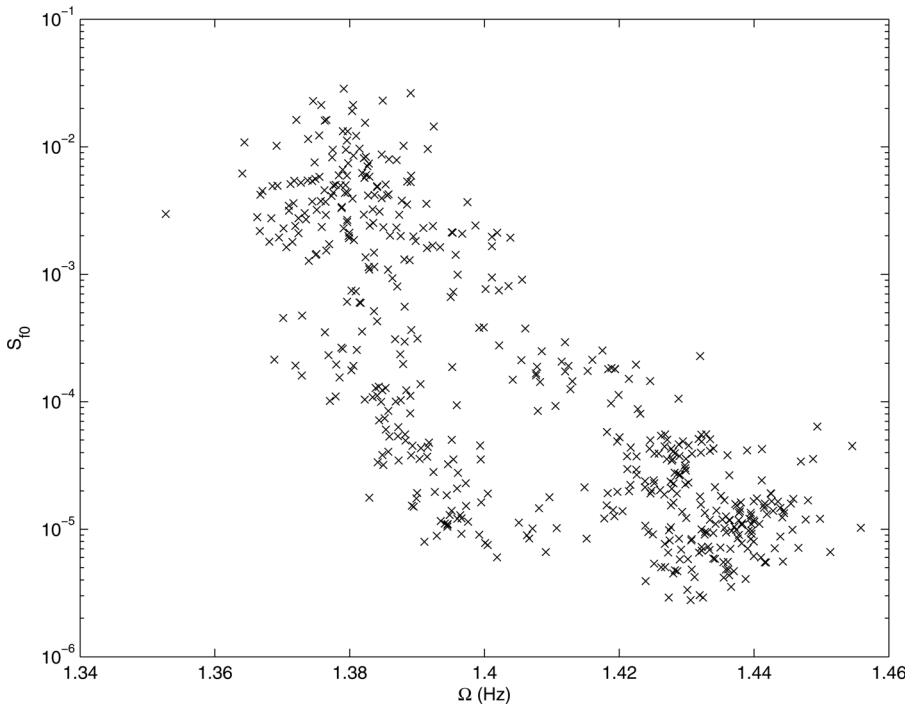

Fig. 9 Identified values of the modal frequency versus spectral intensity

Downloaded 29 Sep 2011 to 161.64.70.118. Redistribution subject to ASME license or copyright; see http://www.asme.org/terms/Terms_Use.cfm

Next, we investigate the modal force spectral intensity and its relationship with the fundamental frequency of the structure. The results presented below are based on those obtained by the Bayesian spectral density approach but similar conclusion can be made using the Bayesian time-domain approach. Figure 8 shows the corresponding spectral intensity of the modal force. Compared with the wind speed shown in Fig. 5, it is observed that the spectral intensity had a similar trend with the root-mean-square of the structural response but not the wind speed. In Fig. 5, the peak of the wind speed occurred at approximately the 19th hour but the peak of the structural acceleration occurred approximately 7 hs later. This confirms that not only the wind speed but also the wind direction affects the magnitude of the structural response. It can be further verified by the fact that the peak of structural response (Fig. 5) and the spectral intensity (Fig. 8) occurred almost at the same time (approximately the 26th hour).

Figure 9 shows the modal frequency versus the spectral intensity of the modal force in the semilogarithmic scale. The modal frequency decreased as the spectral intensity of the modal force increased. In other words, the structural stiffness was degraded when the excitation was at high level. However, there is no evidence for structural damage since such loss was recovered after the typhoon was dissipated. One possible explanation is that the structure went through nonlinear or even hysteretic behavior so the identified modal frequency of the equivalent linear system was reduced [169–172].

8 Conclusion

In this paper, some recently developed Bayesian model updating methods were introduced. Bayesian inference is useful for uncertainty quantification of identification problems. The introduced methods can be categorized into two types: using response measurements and using modal measurements. The Bayesian time-domain approach utilizes an approximated probability density expansion and it can handle both stationary and nonstationary response measurement. The Bayesian spectral density approach and Bayesian fast Fourier transform approach are frequency-domain methods. They make use of the statistical properties of discrete Fourier transform and they can handle stationary response of linear and nonlinear systems. Another model updating method that uses modal measurements was also introduced. An important feature of this approach is that it does not proceed with the commonly required mode matching. This is important as the measured modes are not necessarily the lowest ones and their order may be unknown. An application of a 22-story building subjected to severe typhoon was presented. Reduction of the modal frequency was observed when the wind speed was over 40 km/hr. The comparison could be made because the uncertainty level of the estimation could be quantified. The Bayesian methodology is necessary in this type of application which requires comparison of the identified parameters. Finally, comments were made on the suitability of model class for identification.

Acknowledgment

The authors would like to gratefully acknowledge the generous support by the Research Committee of University of Macau under Grant No. RG059/09-10S/YKV/FST.

References

[1] Eykhoff, P., 1974, *System Identification–Parameter and State Estimation*, Wiley, New York.
[2] Kozin, F., and Natke, H. G., 1986, "System Identification Techniques," Structural Safety, **3**, pp. 269–316.
[3] Natke, H. G., 1988, "Updating Computational Models in the Frequency Domain Based on Measured Data: A Survey," Probab. Eng. Mech., **3**(1), pp. 28–35.
[4] Mottershead, J. E., and Friswell, M. I., 1993, "Model Updating in Structural Dynamics: A Survey," J. Sound Vib., **167**(2), pp. 347–375.
[5] Ghanem, R., and Shinozuka, M., 1995, "Structural-System Identification. I: Theory," J. Eng. Mech., **121**(2), pp. 255–264.
[6] Peeters, B., and De Roeck, G., 2001, "Stochastic System Identification for Operational Modal Analysis: A Review," J. Dyn. Syst., Meas., Control, **123**(4), pp. 659–667.
[7] Hemez, F. M., and Doebling, S. W., 2001, "Review and Assessment of Model Updating for Nonlinear, Transient Dynamics," Mech. Syst. Signal Process., **15**(1), pp. 45–74.
[8] Chang, P. C., Flatau, A., and Liu, S. C., 2003, "Review Paper: Health Monitoring of Civil Infrastructure," Struct. Health Monit., **2**(3), pp. 257–267.
[9] Sohn, H., Farrar, C. R., Hemez, F. M., Shunk, D. D., Stinemates, D. W., and Nadler, B. R., 2003, "A Review of Structural Health Monitoring Literature: 1996-2001," Los Alamos National Laboratory Report No. LA-13976-MS.
[10] Johnson, E. A., Lam, H. F., Katafygiotis, L. S., and Beck, J. L., 2004, "Phase I IASC-ASCE Structural Health Monitoring Benchmark Problem Using Simulated Data," J. Eng. Mech., **130**(1), pp. 3–15.
[11] Kerschen, G., Worden, K., Vakakis, A. F., and Golinval, J. C., 2006, "Past, Present and Future of Nonlinear System Identification in Structural Dynamics," Mech. Syst. Signal Process., **20**(3), pp. 505–592.
[12] Lopez, I., and Sarigul-Klijn, N., 2010, "A Review of Uncertainty in Flight Vehicle Structural Damage Monitoring, Diagnosis and Control: Challenges and Opportunities," Prog. Aerosp. Sci., **46**(7), pp. 247–273.
[13] Brown, D. L, Allemang, R. J., Zimmerman, R., and Mergeay, M., 1979, "Parameters Estimation Techniques for Modal Analysis," Society of Automotive Engineers, Technical Paper No. 790,221.
[14] Doebling, S.W., 1997, "An Overview of Modal-Based Damage Identification Methods, Los Alamos National Laboratory," Los Alamos, NM.
[15] Ren, W. X., and De Roeck, G., 2002, "Structural Damage Identification Using Modal Data. II: Test Verification," J. Struct. Eng., **128**(1), pp. 96–104.
[16] Ivanovíc, S. S., Trifunac, M. D., and Todorovska, M. I., 2000, "Ambient Vibration Tests of Structures - A Review," ISET J. Earthquake Technol., **37**(4), pp. 165–197.
[17] Farrar, C. R., Doebling, S. W., and Nix, D. A., 2001, "Vibration-Based Structural Damage Identification," Philos. Trans. R. Soc. London, Ser. A, **359**(1778), pp. 131–149.
[18] Brownjohn, J. M. W., 2003, "Ambient Vibration Studies for System Identification of Tall Buildings," Earthquake Eng. Struct. Dyn., **32**(1), pp. 71–95.
[19] Kołakowski, P., 2007, "Structural Health Monitoring–A Review With the Emphasis on Low-Frequency Methods," Eng. Trans., **55**(3), pp. 1–37.
[20] Young, P. C., 1970, "An Instrumental Variable Method for Real-Time Identification of a Noisy Process," Automatica, **6**(2), pp. 271–287.
[21] Juang, J. N., and Pappa, R. S., 1985, "An Eigensystem Realization Algorithm for Modal Parameter Identification and Model Reduction," J. Guid. Control Dyn. (AIAA), **8**, pp. 620–627.
[22] Asmussen, J. C., Ibrahim, S. R., and Brincker, R, 1997, "Application of Vector Triggering Random Decrement," Proceedings of 15th International Modal Analysis Conference, Orlando, FL, Vol. 2, pp. 1165–1171.
[23] Worden, K., 1997, "Structural Damage Detection Using a Novelty Measure," J. Sound Vib., **201**(1), pp. 85–101.
[24] Caicedo, J. M., Dyke, S. J., and Johnson, E. A., 2004, "Natural Excitation Technique and Eigensystem Realization Algorithm for Phase I of the IASC-ASCE Benchmark Problem: Simulated Data," J. Eng. Mech., **130**(1), pp. 49–60.
[25] Beck, J. L., May, B. S., and Polidori, D. C., 1994, "Determination of Modal Parameters From Ambient Vibration Data for Structural Health Monitoring," Proceedings of 1st World Conference on Structural Control, Pasadena, CA, pp. TA3: 3–12.
[26] Kim, H. M., Vanhorn, D. A., and Doiron, H. H., 1994, "Free-Decay Time-Domain Modal Identification for Large Space Structures," J. Guid. Control Dyn. (AIAA), **17**(3), pp. 513–519.
[27] Gersch, W., Taoka, G. T., and Liu, R., 1976, "Structural System Parameter Estimation by Two-Stage Least Squares Method," J. Eng. Mech., **102**(5), pp. 883–899.
[28] Conte, J. P., and Kumar, S., 1996, "Statistical System Identification of Structures Using ARMA Models," Proceedings of 7th ASCE Specialty Conference on Probabilistic Mechanics and Structural Reliability, Worcester, MA, pp. 142–145.
[29] Moore, S. M., Lai, J. C. S, and Shankar, K., 2007, "ARMAX Modal Parameter Identification in the Presence of Unmeasured Excitation–I: Theoretical Background," Mech. Syst. Signal Process., **21**(4), pp. 1601–1615.
[30] Goodwin, G. C., and Sin, K. S., 1984, *Adaptive Filtering Prediction and Control*, Prentice-Hall, Englewood Cliffs, NJ.
[31] Ljung, L., 1987, *System Identification: Theory for the User* (Prentice-Hall, Englewood Cliffs, NJ, 1987).
[32] Soderstrom, T., and Stoica, P., 1989, *System Identification*, Prentice-Hall, Englewood Cliffs, NJ.
[33] Beck, J. L., 1978, "Determining Models of Structures from Earthquake Records," Earthquake Engineering Research Laboratory, California Institute of Technology, Pasadena, CA, Technical Report No. EERL 78-01.
[34] Hoshiya, M., and Saito, E., 1984, "Structural Identification by Extended Kalman Filter," J. Eng. Mech., **110**(12), pp. 1757–1770.
[35] Hoshiya, M., 1988, "Application on Extended Kalman Filter-WGI Method in Dynamic System Identification," *Stochastic Structural Dynamics* (Progress in Theory and Application), Elsevier, New York, pp. 103–124.
[36] Juang, J. N., and Suzuki, H., 1988, "An Eigensystem Realization Algorithm in Frequency Domain for Modal Parameter Identification," ASME J. Vib., Acoust., Stress, Reliab. Des., **110**(1), pp, 24–29.

Downloaded 29 Sep 2011 to 161.64.70.118. Redistribution subject to ASME license or copyright; see http://www.asme.org/terms/Terms_Use.cfm

[37] Lin, J. S., and Zhang, Y., 1994, "Nonlinear Structural Identification Using Extended Kalman Filter," Computers and Structures, **52**(4), pp. 757–764.
[38] Koh, C. G., See, L. M., and Balendra, T., 1999, "Determination of Storey Stiffness of Three-Dimensional Frame Buildings," Eng. Struct., **17**(3), pp. 179–186.
[39] Lus, H., Betti, R., and Longman, R. W., 1999, "Identification of Linear Structural Systems Using Earthquake-Induced Vibration Data," Earthquake Eng. Struct. Dyn., **28**(11), pp. 1449–1467.
[40] Quek, S. T., Wang, W., and Koh, C. G., 1999, "System Identification of Linear MDOF Structures Under Ambient Excitation," Earthquake Eng. Struct. Dyn., **28**(1), pp. 61–77.
[41] Shi, T., Jones, N. P., and Ellis, J. H., 2000, "Simultaneous Estimation of System and Input Parameters From Output Measurements," J. Eng. Mech., **126**(7), pp. 746–753.
[42] Lus, H., Betti, R., and Longman, R. W., 2002, "Obtaining Refined First-Order Predictive Models of Linear Structural Systems," Earthquake Eng. Struct. Dyn., **31**(7), pp. 1413–1440.
[43] Lin, J. W., and Betti, R., 2004, "Online Identification and Damage Detection in Nonlinear Structural Systems Using a Variable Forgetting Factor Approach," Earthquake Eng. Struct. Dyn., **33**(4), pp. 419–444.
[44] Papadimitriou, C., Fritzen, C. P., Kraemer, P., and Ntotsios, E., 2011, "Fatigue Predictions in Entire Body of Metallic Structures from a Limited Number of Vibration Sensors Using Kalman Filtering," Struct. Control Health Monit., **18**.
[45] Feldman, M., 1994, "Nonlinear System Vibration Analysis Using Hilbert Transform-II. Forced Vibration Analysis Method 'FORCEVIB'," Mech. Syst. Signal Process., **8**(3), pp. 309–318.
[46] Kitada, Y., 1998, "Identification of Nonlinear Structural Dynamic Systems Using Wavelets," J. Eng. Mech., **124**(10), pp. 1059–1066.
[47] Zeldin, B. A., and Spanos, P. D., 1998, "Spectral Identification of Nonlinear Structural Systems," J. Eng. Mech., **124**(7), pp. 728–733.
[48] Saadat, S., Buckner, G. D., Furukawa, T., and Noori, M. N., 2004, "An Intelligent Parameter Varying (IPV) Approach for Nonlinear System Identification of Base Excited Structures," Int. J. Non–Linear Mech., **39**(6), pp. 993–1004.
[49] Pilipchuk, V. N., and Tan, C. A., 2005, "Nonlinear System Identification Based on Lie Series Solutions," Mech. Syst. Signal Process., **19**(1), pp. 71–86.
[50] Ashrafi, S. A., Smyth, A. W., and Betti, R., 2006, "A Parametric Identification Scheme for Nondeteriorating and Deteriorating Nonlinear Hysteretic Behavior," Struct. Control Health Monit., **13**, pp. 108–131.
[51] Roberts, J. B., Dunne, J. F., and Debonos, A., 1995, "A Spectral Method for Estimation for Nonlinear System Parameters From Measured Response," Probab. Eng.Mech., **10**(4), pp. 199–207.
[52] Coca, D., and Billings, S. A., 2001, "Nonlinear System Identification Using Wavelet Multiresolution Models," Int. J. Control, **74**(18), pp. 1718–1736.
[53] Chen, Q., Chan, Y. W., and Worden, K., 2003, "Structural Fault Diagnosis and Isolation Using Neural Networks Based on Response-Only Data," Computers and Structures, **81**(22–23), pp. 2165–2172.
[54] Hickey, D., Worden, K., Platten, M. F., Wright, J. R., and Cooper, J. E., 2009, "Higher-Order Spectra for Identification of Nonlinear Modal Coupling," Mech. Syst. Signal Process., **23**(4), pp. 1037–1061.
[55] Beck, J. L., 1990, "Statistical System Identification of Structures," *Structural Safety and Reliability*, ASCE, New York, pp. 1395–1402.
[56] Sohn, H., and Law, K. H., 1997, "A Bayesian Probabilistic Approach for Structure Damage Detection," Earthquake Eng. Struct. Dyn., **26**(12), pp. 1259–1281.
[57] Yun, C. B., and Lee, H. J., 1997, "Substructural Identification for Damage Estimation of Structures," Structural Safety, **19**(1), pp. 121–140.
[58] Beck, J. L. and Katafygiotis, L. S., 1998, "Updating Models and Their Uncertainties. I: Bayesian Statistical Framework," J. Eng. Mech. (ASCE), **124**(4), pp. 455–461.
[59] Katafygiotis, L. S., Papadimitriou, C., and Lam, H. F., 1998, "A Probabilistic Approach to Structural Model Updating," Soil Dyn. Earthquake Eng., **17**(7–8), pp. 495–507.
[60] Enright, M. P., and Frangopol, D. M., 1999, "Condition Prediction of Deteriorating Concrete Bridges Using Bayesian Updating," J. Struct. Eng., **125**(10), pp. 1118–1125.
[61] Sohn, H., and Law, K. H., 2000, "Bayesian Probabilistic Damage Detection of a Reinforced-Concrete Bridge Column," Earthquake Eng. Struct. Dyn., **29**, pp. 1131–1152.
[62] Kerschen, G., Golinval, J. C., and Hemez, F. M., 2003, "Bayesian Model Screening for the Identification of Nonlinear Mechanical Structures," J. Vibr. Acoust., **125**(3), pp. 389–397.
[63] Estes, A. C., Frangopol, D. M., and Foltz, S. D., 2004, "Updating Reliability of Steel Miter Gates on Locks and Dams Using Visual Inspection Results," Eng. Struct., **26**(3), pp. 319–333.
[64] Yuen, K. V., Au, S. K., and Beck, J. L., 2004, "Two-Stage Structural Health Monitoring Methodology and Results for Phase I Benchmark Studies," J. Eng. Mech., **130**(1), pp. 16–33.
[65] Bucher, C., and Pham, H. A., 2005, "On Model Updating of Existing Structures Utilizing Measured Dynamic Responses," Struct. Infrastruct. Eng., **1**(2), pp. 135–143.
[66] Ching, J., Beck, J. L., Porter, K. A., and Shaikhutdinov, R., 2006, "Bayesian State Estimation Method for Nonlinear Systems and Its Application to Recorded Seismic Response," J. Eng. Mech., **132**(4), pp. 396–410.
[67] Porter, K., Mitrani-Reiser, J., and Beck, J. L., 2006, "Near-Real-Time Loss Estimation for Instrumented Buildings," Struct. Des. Tall Spec. Build., **15**(1), pp. 3–20.
[68] Wu, J. R., and Li, Q. S., 2006, "Structural Parameter Identification and Damage Detection for a Steel Structure Using a Two-Stage Finite Element Model Updating Method," J. Constr. Steel Res., **62**(3), pp. 231–239.
[69] Bezazi, A., Pierce, S. G., Worden, K., and Harkati, E. H., 2007, "Fatigue Life Prediction of Sandwich Composite Materials Under Flexural Tests Using a Bayesian Trained Artificial Neural Network," Int. J. Fatigue, **29**(4), pp. 738–747.
[70] Gardoni, P., Nemati, K. M., and Noguchi, T., 2007, "Bayesian Statistical Framework to Construct Probabilistic Models for the Elastic Modulus of Concrete," J. Mater. Civ. Eng., **19**(10), pp. 898–905.
[71] Gardoni, P., Reinschmidt, K. F., and Kumar, R., 2007, "A Probabilistic Framework for Bayesian Adaptive Forecasting of Project Progress," Comput. Aided Civ. Infrastruct. Eng., **22**(3), pp. 182–196.
[72] Jiang, X., Mahadevan, S., and Adeli, H., 2007, "Bayesian Wavelet Packet Denoising for Structural System Identification," Struct. Control Health Monit., **14**(2), pp. 333–356.
[73] Yuen, K. V., Hoi, K. I., and Mok, K. M., 2007, "Selection of Noise Parameters for Kalman Filter," Earthquake Eng. Eng. Vib., **6**(1), pp. 49–56.
[74] Christodoulou, K., Ntotsios, E., Papadimitriou, C., and Panetsos, P., 2008, "Structural Model Updating and Prediction Variability Using Pareto Optimal Models," Comput. Methods Appl. Mech. Eng., **198**(1), pp. 138–149.
[75] Pierce, S. G., Worden, K., and Bezazi, A., 2008, "Uncertainty Analysis of a Neural Network Used for Fatigue Lifetime Prediction," Mech. Syst. Signal Process., **22**(6), pp. 1398–1411.
[76] Chen, Y. B., Feng, M. Q., and Tan, C. A., 2009, "Bridge Structural Condition Assessment Based on Vibration and Traffic Monitoring," J. Eng. Mech. **135**(8), pp. 747–758.
[77] Cetin, K. O. and Ozan, C., 2009, "CPT-Based Probabilistic Soil Characterization and Classification," J. Geotech. Geoenviron. Eng. **135**(1), pp. 84–107.
[78] Cheung, S. H. and Beck, J. L., 2009, "Bayesian Model Updating Using Hybrid Monte Carlo Simulation With Application to Structural Dynamic Models With Many Uncertain Parameters," J. Eng. Mech., **135**(4), pp. 243–255.
[79] Worden, K., Manson, G., and Denceux, T., 2009, "An Evidence-Based Approach to Damage Location on an Aircraft Structure," Mech. Syst. Signal Process., **23**(6), pp. 1792–1804.
[80] Raphael, W., Faddoul, R., Selouan, D. E. A., and Chateauneuf, A., 2009, "Information-Based Information for Bayesian Updating of the Eurocode 2 Creep Model," Structural Concrete, **10**(2), pp. 55–62.
[81] Straub, D., 2009, "Stochastic Modeling of Deterioration Processes Through Dynamic Bayesian Networks," J. Eng. Mech., **135**(10), pp. 1089–1099.
[82] Zhang, J., Zhang, L. M., and Tang, W. H., 2009, "Bayesian Framework for Characterizing Geotechnical Model Uncertainty," J. Geotech. Geoenviron. Eng., **135**(7), pp. 932–940.
[83] Fraccone, G. C., Volovoi, V., and Ruzzene, M., 2010, "Bayesian Estimation of a Dynamic Structure's Response," J. Sound Vib., **329**(1), pp. 21–42.
[84] Jalayer, F., Iervolino, I., and Manfredi, G., 2010, "Structural Modeling Uncertainties and Their Influence on Seismic Assessment of Existing RC Structures," Structural Safety, **32**(3), pp. 220–228.
[85] Radhika, B., and Manohar, C. S., 2010, "Reliability Models for Existing Structures Based on Dynamic State Estimation and Data Based Asymptotic Extreme Value Analysis," Probab. Eng. Mech., **25**(4), pp. 393–405.
[86] Soyoz, S., Feng, M. Q., and Shinozuka, M., 2010, "Structural Reliability Estimation With Vibration-Based Identified Parameters," J. Eng. Mech., **136**(1), pp. 100–106.
[87] Yuen, K. V., 2010, *Bayesian Methods for Structural Dynamics and Civil Engineering*, Wiley, New York.
[88] Jaynes, E. T., "Bayesian Methods: General Background," *Maximum Entropy and Bayesian Methods in Applied Statistics* (Cambridge University Press, New York, 1986), pp. 1–25.
[89] Box, G. E. P., and Tiao, G. C., *Bayesian Inference in Statistical Analysis* (Wiley, New York, 1992).
[90] Papadimitriou, C., Katafygiotis, L. S., and Au, S. K., 1997, "Effects of Structural Uncertainties on TMD Design: A Reliability-Based Approach," J. Struct. Control, **4**(1), pp. 65–88.
[91] Yuen, K. V., and Beck, J. L., 2003, "Reliability-Based Robust Control for Uncertain Dynamical Systems Using Feedback of Incomplete Noisy Measurements," Earthquake Eng. Struct. Dyn., **32**(5), pp. 751–770.
[92] Yuen, K. V., Shi, Y. F., Beck, J. L., and Lam, H. F., 2007, "Structural Protection Using MR Dampers With Clipped Robust Reliability-Based Control," Struct. Multidiscip. Optim., **34**(5), pp. 431–443.
[93] Lin, Y. K., 1976, *Probabilistic Theory of Structural Dynamics*, Robert E. Krieger Pub. Co., Malabar, FL.
[94] Lutes, L. D., and Sarkani, S., 1997, *Stochastic Analysis of Structural and Mechanical Vibrations*, Prentice-Hall, Englewood Cliffs, NJ.
[95] Koh, C. G., Chen, Y. F., and Liaw, C. Y., 2003, "A Hybrid Computational Strategy for Identification of Structural Parameters," Computers and Structures, **81**(2), pp. 107–117.
[96] Yu, J., Imbimbo, M., and Betti, R., 2009, "Identification of Linear Structural Systems With a Limited Set of Input-Output Measurements," ASME J. Appl. Mech., **76**(3), pp. 031005-1–031005-10.
[97] Ljung, L., and Glad, T., 1994, "On Global Identifiability of Arbitrary Model Parameterizations," Automatica, **30**(2), pp. 265–276.
[98] Katafygiotis, L. S. and Beck, J. L., 1998, "Updating Models and Their Uncertainties. II: Model Identifiability," J. Eng. Mech., **124**(4), pp. 463–467.
[99] Jaynes, E. T., 1978, *Where Do We Stand on Maximum Entropy?*, MIT Press, Cambridge, MA.
[100] Papadimitriou, C., Beck, J. L. and Au, S. K., 2000, "Entropy-Based Optimal Sensor Location for Structural Model Updating," J. Vib. Control, **6**(5), pp. 781–800.
[101] Yuen, K. V., Katafygiotis, L. S., Papadimitriou, C., and Mickleborough, N. C., 2001, "Optimal Sensor Placement Methodology for Identification With

Downloaded 29 Sep 2011 to 161.64.70.118. Redistribution subject to ASME license or copyright; see http://www.asme.org/terms/Terms_Use.cfm

Unmeasured Excitation," ASME J. Dyn. Syst., Meas., Control, **123**(4), pp. 677–686.
[102] Papadimitriou, C., 2004, "Optimal Sensor Placement Methodology for Parametric Identification of Structural Systems," J. Sound Vib., **278**(4/5), pp. 923–947.
[103] Papadimitriou, C., 2005, "Pareto Optimal Sensor Locations for Structural Identification," Comput. Methods Appl. Mech. Eng., **194**(12–16), pp. 1655–1673.
[104] Chow, H. M., Lam, H. F., Yin, T., and Au, S. K., 2011, "Optimal Sensor Configuration of a Typical Transmission Tower for the Purpose of Structural Model Updating," Struct. Control Health Monit., **18**(3), pp. 305–320.
[105] Mackay, D. J. C., 1992, "Bayesian Interpolation," Neural Comput., **4**(3), pp. 415–447.
[106] Mark, J. L., 1995, "Regularization in the Selection of Radial Basis Function Centers," Neural Comput., **7**(3), pp. 606–623.
[107] Yuen, K. V., and Katafygiotis, L. S., 2002, "Bayesian Modal Updating Using Complete Input and Incomplete Response Noisy Measurements," J. Eng. Mech., **128**(3), pp. 340–350.
[108] Yuen, K. V., Beck, J. L., and Katafygiotis, L. S., 2006, "Unified Probabilistic Approach for Model Updating and Damage Detection," J. Appl. Mech., **73**(4), pp. 555–564.
[109] Yuen, K. V., and Katafygiotis, L. S., 2001, "Bayesian Time-Domain Approach for Modal Updating Using Ambient Data," Probab. Eng. Mech., **16**(3), pp. 219–231.
[110] Yuen, K. V., Beck, J. L., and Katafygiotis, L. S., 2002, "Probabilistic Approach for Modal Updating Using Nonstationary Noisy Response Measurements Only," Earthquake Eng. Struct. Dyn., **31**(4), pp. 1007–1023.
[111] Brockwell, P. J., and Davis, R. A., 1991, *Time Series: Theory and Methods*, Springer-Verlag, New York.
[112] Katafygiotis, L. S., and Yuen, K. V., 2001, "Bayesian Spectral Density Approach for Modal Updating Using Ambient Data," Earthquake Eng. Struct. Dyn., **30**(8), pp. 1103–1123.
[113] Matlab, 1994, *Matlab User's Guide*, MathWorks, Inc., Natick, MA.
[114] Krishnaiah, P. R., 1976, "Some Recent Developments on Complex Multivariate Distributions," J. Multivariate Anal., **6**(1), pp. 1–30.
[115] Yuen, K. V., Katafygiotis, L. S., and Beck, J. L., 2002, "Spectral Density Estimation of Stochastic Vector Processes," Probab. Eng. Mech., **17**(3), pp. 265–272.
[116] Yuen, K. V., and Beck, J. L., 2003, "Updating Properties of Nonlinear Dynamical Systems With Uncertain Input," J. Eng. Mech., **129**(1), pp. 9–20.
[117] Yuen, K. V., and Katafygiotis, L. S., 2003, "Bayesian Fast Fourier Transform Approach for Modal Updating Using Ambient Data," Adv. Struct. Eng., **6**(2), pp. 81–95.
[118] Yuen, K. V., and Katafygiotis, L. S., 2005, "Model Updating Using Noisy Response Measurements Without Knowledge of the Input Spectrum," Earthquake Eng. Struct. Dyn., **34**(2), pp. 167–187.
[119] Koh, C. G., See, L. M., and Balendra, T., 1991, "Estimation of Structural Parameters in Time Domain: A Substructure Approach," Earthquake Eng. Struct. Dyn., **20**(8), pp. 787–801.
[120] Koh, C. G., and Shankar, K., 2003, "Substructural Identification Method Without Interface Measurement," J. Eng. Mech., **129**(7), pp. 769–776.
[121] Tee, K. F., Koh, C. G., and Quek, S. T., 2009, "Numerical and Experimental Studies of a Substructural Identification Strategy," Struct. Health Monit., **8**(6), pp. 574–574.
[122] Yuen, K. V., and Katafygiotis, L. S., 2006, "Substructure Identification and Health Monitoring Using Response Measurement Only," Computer-Aided Civ. Infrastruct. Eng., **21**(4), pp. 280–291.
[123] Berman, A., 1979, "Mass Matrix Correction Using an Incomplete Set of Measured Modes," AIAA J., **17**(10), pp. 1147–1148.
[124] Kabe, A. M., 1985, "Stiffness Matrix Adjustment Using Mode Data," AIAA J., **23**(9), pp. 1431–1436.
[125] Wei, F. S., 1990, "Analytic Dynamic Model Improvement Using Vibration Test Data," AIAA J., **28**(1), pp. 175–177.
[126] Farhat, C., and Hemez, F. M., 1993, "Updating Finite Element Dynamics Models Using Element-by-Element Sensitivity Methodology," AIAA J., **31**(9), pp. 1702–1711.
[127] Pandey, A. K., and Biswas, M., 1995, "Experimental Verification of Flexibility Difference Method for Locating Damage in Structures," J. Sound Vib., **184**, pp. 311–328.
[128] Bernal, D., 2002, "Load Vectors for Damage Localization," J. Eng. Mech., **128**(1), pp. 7–14.
[129] Yuen, K. V., 2010, "Efficient Model Correction Method With Modal Measurement," J. Eng. Mech., **136**(1), pp. 91–99.
[130] Hearn, G. and Testa, R. B., 1991, "Modal Analysis for Damage Detection in Structures," J. Struct. Eng., **117**(10), pp. 3042–3063.
[131] Friswell, M. I., and Mottershead, J. E., 1995, *Finite Element Model Updating in Structural Dynamics*, Kluwer Academic Publishers, Boston.
[132] Doebling, S. W., Farrar, C. R., and Prime, M. B., 1998, "A Review of Damage Identification Methods That Examine Changes in Dynamics Properties," Shock Vib., **30**(2), pp. 91–105.
[133] Sanayei, M., McClain, J. A. S., Wadia-Fascetti, S., and Santini, E. M., 1999, "Parameter Estimation Incorporating Modal Data and Boundary Conditions," J. Struct. Eng., **125**(9), pp. 1048–1055.
[134] Smyth, A. W., Masri, S. F., Caughey, T. K., and Hunter, N. F., 2000, "Surveillance of Intricate Mechanical Systems on the Basis of Vibration Signature Analysis," ASME J. Appl. Mech., **67**(3), pp. 540–551.
[135] Allemang, R. J., 2003, "The Modal Assurance Criterion: Twenty Years of Use and Abuse," Sound and Vibration Magazine, **37**(8), pp. 14–23.
[136] Beck, J. L., Au, S. K., and Vanik, M. W., 2001, "Monitoring Structural Health Using a Probabilistic Measure," Computer-Aided Civil and Infrastructure Engineering, **16**(1), pp. 1–11.
[137] Ching, J., and Beck, J. L., 2004, "New Bayesian Model Updating Algorithm Applied to a Structural Health Monitoring Benchmark," Struct. Health Monit., **3**(4), pp. 313–332.
[138] Ntotsios, E., Papadimitriou, C., Panetsos, P., Karaiskos, G., Perros, K, and Perdikaris, P., 2009, "Bridge Health Monitoring System Based on Vibration Measurements," Bull. Earthquake Eng., **7**(2), pp. 469–483.
[139] Yuen, K. V., Beck, J. L., and Katafygiotis, L. S., 2006, "Efficient Model Updating and Monitoring Methodology Using Incomplete Modal Data Without Mode Matching," Struct Control Health Monit., **13**(1), pp. 91–107.
[140] Zellner, A., Keuzenkamp, H. A., and McAleer, M., 2001, *Simplicity, Inference and Modeling: Keeping it Sophisticatedly Simple*, Cambridge University, Cambridge.
[141] Cox, R. T., 1961, *The Algebra of Probable Inference*, John Hopkins Univ. Press, Balitmore, MD.
[142] Jeffreys, H., 1961, *Theory of Probability*, 3rd ed., Clarendon, Oxford, UK.
[143] Beck, J. L. and Yuen, K. V., 2004, "Model Selection Using Response Measurements: Bayesian Probabilistic Approach," J. Eng. Mech., **130**(2), pp. 192–203.
[144] Yuen, K. V., 2010, "Recent Developments of Bayesian Model Class Selection and Applications in Civil Engineering," Structural Safety, **32**(5), pp. 338–346.
[145] Papadimitriou, C., Beck, J. L., and Katafygiotis, L. S., 1997, "Asymptotic Expansions for Reliability and Moments of Uncertain Systems," J. Eng. Mech., **123**(12), pp. 1219–1229.
[146] Gull, S. F., 1988, "Bayesian Inductive Inference and Maximum Entropy," *Proceedings of Maximum Entropy and Bayesian Methods in Science and Engineering*, G. J. Erickson and C. R. Smith, eds., Kluwer Academic Publishers, Dordrecht, Vol. **1**, pp. 53–74.
[147] Yuen, K. V. and Lam, H. F., 2006, "On the Complexity of Artificial Neural Networks for Smart Structures Monitoring," Eng. Struct., **28**(7), pp. 977–984.
[148] Lam, H. F., Yuen, K. V., and Beck, J. L., 2006, "Structural Health Monitoring via Measured Ritz Vectors Utilizing Artificial Neural Networks," Computer-Aided Civil and Infrastructure Engineering, **21**(4), pp. 232–241.
[149] Yamada, M., Heaton, T., and Beck, J. L., 2007, "Real-Time Estimation of Faulty Rupture Extent Using Near-Source Versus Far-Source Classification," Bull. Seismol. Soc. Am., **97**(6), pp. 1890–1910.
[150] Muto, M., and Beck, J. L., 2008, "Bayesian Updating and Model Class Selection for Hysteretic Structural Models Using Stochastic Simulation," J. Vib. Control, **14**(1-2), pp. 7–34.
[151] Hoi, K. I., Yuen, K. V., and Mok, K. M., 2009, "Prediction of Daily Averaged PM_{10} Concentrations by Statistical Time-Varying Model," Atmos. Environ., **43**(16), pp. 2579–2581.
[152] Yan, W. M., Yuen, K. V., and Yoon, G. L., 2009, "Bayesian Probabilistic Approach for the Correlations of Compressibility Index for Marine Clays," J. Geotech. Geoenviron. Eng., **135**(12), pp. 1932–1940.
[153] Wolf, M. T. and Burdick, J. W., 2009, "A Bayesian Clustering Method for Tracking Neural Signals Over Successive Intervals," IEEE Trans. Biomed. Eng., **56**(11), pp. 2649–2659.
[154] Yuen, K.V., and Kuok, S. C., 2010, "Modeling of Environmental Influence in Structural Health Monitoring Assessment for Reinforced Concrete Buildings," Earthquake Eng. Eng. Vib., **9**(2), pp. 295–306.
[155] Arangio, S., Bontempi, F., and Ciampoli, M., 2011, "Structural Integrity Monitoring for Dependability," Struct. Infrastruct. Eng., **7**(12), pp. 75–86.
[156] Lam, H. F., and Yin, T., 2010, "Statistical Detection of Multiple Cracks on Thin Plates Utilizing Dynamic Response," Eng. Struct., **32**(10), pp. 3145–3152.
[157] Gaitanaros, S., Karaiskos, G., Papadimitriou, C., and Aravas, N., 2010, "A Bayesian Methodology for Crack Identification in Structures Using Strain Measurements," Int. J. Reliab. Safety, **4**(2/3), pp. 206–237.
[158] Yuen, K. V., and Mu, H. Q., 2011, "Peak Ground Acceleration Estimation by Linear and Nonlinear Models With Reduced Order Monte Carlo Simulation," Computer-Aided Civil and Infrastructure Engineering, **26**(11), pp. 30–47.
[159] Ching, J., and Chen, Y. C., 2007, "Transitional Markov Chain Monte Carlo Method for Bayesian Model Updating, Model Class Selection and Model Averaging," J. Eng. Mech., **133**(7), pp. 816–832.
[160] Dalgliesh, W. A., Cooper, K. R., and Templin, J. T., 1983, "Comparison of Model and Full-Scale Accelerations of a High Rise Building," J. Wind. Eng. Ind. Aerodyn., **13**(1–3), pp. 217–228.
[161] Xu, Y. L., Chen, S. W., and Zhang, R. C., 2003, "Modal Identification of Di Wang Building Under Typhoon York Using the Hilbert-Huang Transform Method," Struct. Des. Tall Spec. Build., **12**(1), pp. 21–47.
[162] Kijewski, T., Kilpatrick, J., Kareem, A., Kwon, D. K., Bashor, R., Kochly, M., Young, B. S., Abdelrazaq, A., Galsworthy, J., Isyumov, N., Morrish, D., Sinn, R. C., and Baker, W. F., 2006, "Validating the Wind-Induced Response of Tall Buildings: A Synopsis of the Chicago Full-Scale Monitoring Program," J. Struct. Eng., **132**(10), pp. 1509–1523.
[163] Li, Q. S., Xiao, Y. Q., Wu, J. R., Fu, J. Y., and Li, Z. N., 2008, "Typhoon Effects on Super-Tall Buildings," J. Sound Vib., **313**(3–5), pp. 581–602.
[164] Khanduri, A. C., Stathopoulos, T., and Bédard, C., 1998, "Wind-Induced Interference Effects on Buildings-A Review of the State-of-Art," Eng. Struct., **20**(7), pp. 617–630.
[165] John, D. H., 2001, *Wind Loading of Structures*, Spon Press, London.
[166] Ishizaki, H., 1983, "Wind Profiles, Turbulence Intensities and Gust Factors for Design in Typhoon-Prone Regions," J. Wind. Eng. Ind. Aerodyn., **13**(1–3), pp. 55–66.

Downloaded 29 Sep 2011 to 161.64.70.118. Redistribution subject to ASME license or copyright; see http://www.asme.org/terms/Terms_Use.cfm

[167] Chen, J., and Xu, Y. L., 2004, "On Modeling of Typhoon-Induced Nonstationary Wind Speed for Tall Buildings," Struct. Des. Tall Spec. Build., **13**(2), pp. 145–163.
[168] Yuen, K. V., and Kuok, S. C., 2010, "Ambient Interference in Long-Term Monitoring of Buildings," Eng. Struct., **32**(8), pp. 2379–2386.
[169] Iwan, W. D., and Mason, A. B., Jr., 1980, "Equivalent Linearization for Hysteretic Systems Under Random Excitation," ASME J. Appl. Mech., **47**, pp. 150–154.
[170] Baber, T. T., and Wen, Y. K., 1981, "Random Vibration of Hysteretic Degrading Systems," J. Eng. Mech., **107**(6), pp. 1069–1087.
[171] Sues, R. H., Mau, S. T., and Wen, Y. K., 1988, "Systems Identification of Degrading Hysteretic Restoring Forces," J. Eng. Mech., **114**(5), pp. 833–846.
[172] Tamura, Y., and Suganuma, S., 1996, "Evaluation of Amplitude–Dependent Damping and Natural Frequency of Buildings During Strong Winds," J. Wind. Eng. Ind. Aerodyn., **59**(2–3), pp. 115–130.

Downloaded 29 Sep 2011 to 161.64.70.118. Redistribution subject to ASME license or copyright; see http://www.asme.org/terms/Terms_Use.cfm